



**Phytochemical Profile and
Antibacterial - AntiQuorum Sensing
Properties of *Citrus medica* L.**

Hatice Hilal Gunes
Ebru Onem

**Amino Acid Supported Conductive
Nanocomposite for Developing Flexible
Electrode Material for Energy Storage**

Sinem Ortaboy
Melisa Ogretici
Kibar Aras
Elif Caliskan Salihi

**The Antioxidative and
Antimicrobial Activity of
2-Amino Substituted
Halochalcone *N*-glycoside
Derivative Compounds**

Rezzan Aliyazicioglu
Merve Yikilmaz Seyda
Kanbolat Merve
Badem
Seda Fandakli Sengul
Alpay Karaoglu

01

Volume **1**

Issue **3**

October **2024**



Editorial Team

Editor in Chief

Ozlem Bingol Ozakpinar

Vice Editor

Derya Ozsavci

Associate Editors

Turgut Sekerler
Merve Gurboga

Editorial Board Member

Ali Zarrabi

(Istinye University, Faculty of Engineering and Natural Sciences)

Asim Orem

(Karadeniz Technical University, Faculty of Medicine)

Didem

Deliorman Orhan

(Gazi University, Faculty of Pharmacy)

Ebru Alturfan

(Marmara University, Faculty of Dentistry)

Gulgun Tinaz

(Marmara University, Faculty of Pharmacy)

Gulsah Gedik

(Trakya University, Faculty of Pharmacy)

Ilhan Yaylim

(Istanbul University, DETAM)

Turgut Taskin

(Marmara University, Faculty of Pharmacy)

Advisory Board

Deniz Demirci

(Uskudar University, Faculty of Health Sciences)

Elif Caliskan Salihi

(Marmara University, Faculty of Pharmacy)

Engin Kaptan

(Istanbul University, Faculty of Science, Turkey)

Faruk Aydin

(Atlas University, Faculty of Medicine, Turkey)

Gulderen Yanikkaya Demirel

(Yeditepe University, Faculty of Medicine)

Koray Gumustas

(Istanbul-Cerrahpasa University, Faculty of Medicine, Turkey)

Kubra Elcioglu

(Marmara University, Faculty of Pharmacy, Turkey)

Mahfuz Elmastas

(University of Health Sciences, Faculty of Pharmacy, Turkey)

Mehmet Tevfik Dorak

(Kingston University London, Department of Life Sciences, Pharmacy & Chemistry, United Kingdom)

Meltem Yalinay

(Gazi University, Faculty of Medicine, Ankara)

Mohammed Sebahia

(University Hassiba Benbouali of Chlef, Department of Biologie, Algeria)

Tugba Akbay

(Marmara University, Faculty of Dentistry)

Tunc Catal

(Uskudar University, Faculty of Engineering and Natural Sciences)

Sinem Ortaboy Sezer

(Istanbul University, Faculty of Engineering, Turkey)

Yusuf Tutar

(Recep Tayyip Erdogan University, Faculty of Health Sciences, Turkey)

Language Editor

Pervin Rayaman

Publisher

Ismail Celik



CONTENTS

Original Articles

- Phytochemical Profile and Antibacterial-AntiQuorum Sensing Properties of *Citrus medica* L.....102**
Hatice Hilal Gunes, Ebru Onem
- Amino Acid Supported Conductive Nanocomposite for Developing Flexible Electrode Material for Energy Storage.....110**
Sinem Ortaboy, Melisa Ogretici, Kibar Aras, Elif Caliskan Salihi
- The Antioxidative and Antimicrobial Activity of 2-Amino Substituted Halochalcone *N*-glycoside Derivative Compounds.....121**
Rezzan Aliyazicioglu, Merve Yikilmaz, Seyda Kanbolat, Merve Badem, Seda Fandakli, Sengul Alpay Karaoglu



Original Article

Phytochemical Profile and Antibacterial-AntiQuorum Sensing Properties of *Citrus medica* L.

Hatice Hilal Gunes¹ , Ebru Onem¹ 

¹Suleyman Demirel University, Faculty of Pharmacy, Department of Pharmaceutical Microbiology, Isparta, Türkiye

 Corresponding Author: Ebru ONEM (E-mail: ebruonem@sdu.edu.tr)

Received: 2024.09.30; Revised: 2024.10.19; Accepted: 2024.10.23

Abstract

Introduction: Natural resources are becoming more and more important as the need to find solutions to the antibiotic resistance growing crisis. The assessment of medicinal plants' antibacterial and anti-quorum-sensing properties is gaining popularity in this field of research every day. The study reported here aimed to investigate the inhibitory activity of the methanolic extract of *Citrus medica* L. on the inhibition of violacein pigment production in *Chromobacterium violaceum* ATCC 12472 and some virulence factors in *Pseudomonas aeruginosa* PAO1. Additionally the phenolic content of the extract was also determined by HPLC analysis.

Methods: The phytochemical content of the plant extract was determined and its antibacterial activity on some bacteria was tested. Also antibiofilm effect on PAO1 was determined, and violacin pigment inhibition on *C. violaceum* was investigated.

Results: It was observed that the methanolic extract had an inhibition effect of 32% on violacein pigment production and a strong inhibition effect of 88% on biofilm formation caused by PAO1. According to the results of the phytochemical content analysis, benzoic acid was determined as the major component of the extract with a concentration value of 41.9 µg/mL.

Conclusion: *Citrus medica* L, like many plants, has antibacterial and anti-quorum sensing activity and may be a potential agent in the fight against infectious diseases.

Keywords: Anti-quorum sensing, Citrus, phytochemical, PAO1, violacein

1. Introduction

Long-term use of antibiotics in the treatment of bacterial infections causes some undesirable side effects and infections resistant to antibiotic treatment. Resistance is not limited to one drug, but is seen in many drugs and appears as multiple antibiotic resistance. This prolongs the duration of

treatment and increases the length of hospitalization. It also increases the investment and cost of health services (1).

The fact that all these problems also threaten public health pushed scientists to search for different solutions, especially natural solutions of plant origin (2). Plants generally have antioxidant effect

and capacity against free radicals that can cause irreversible damage to important compounds such as carbohydrates, lipids, proteins, nucleic acids and DNA in our body. Plants show this effect by preventing the formation of reactive oxygen species, neutralizing free radicals and detoxifying radicals by converting them into more harmless compounds (3). Phenolic compounds found in the roots, leaves and above-ground tissues of plants used for many purposes among the people, which provide many properties such as antimicrobial, anti-inflammatory and anticancer, and the components in their essential oils. The determination of the existence of plant ingredients on scientific grounds has increased the trust in plants and is seen as one of the options that can be evaluated in the fight against infectious diseases. In addition, another option is to prevent bacteria from communicating with other bacteria, which is different from the antibacterial effect (4). The discovery that many pathogenic bacteria produce virulence factors that are effective in the development of successful infection process through the quorum sensing (QS) system has made this system a therapeutic target for the design and development of a new class of drugs that potentially control pathogenicity (5).

The QS mechanism depends on the synthesis, release and uptake of autoinducers (AIs) in the surrounding environment, the concentration of which is related to the density of secreting bacteria. AIs, extracellular signaling molecules that accumulate in the environment in proportion to cell density, are used for this intercellular communication. Their function is to regulate gene expression in other cells of the community and control a range of bacterial responses. QS systems have been present in bacteria since time immemorial, and since ancient times bacteria have regulated a variety of cellular functions through their QS machinery, including luminescence, biofilm formation, sporulation, development of genetic competence, synthesis of peptide antibiotics, production of secreted proteolytic enzymes, virulence factor expression, pigment production, plant-microbe interactions and motility (6). Disruption of this communication system or bacterial QS activity leads to attenuation of the

microbial virulence.

Inactivation or disruption of QS signaling molecules is known as QS inhibition or quorum quenching. This inhibition can be achieved by various means, such as the development of antibodies against QS signaling molecules, enzymatic degradation of QS signaling molecules or agents that block QS. These strategies interfere with the cell-to-cell communication system and monitor the growth of infectious bacteria without stopping them, thus preventing the development of antibiotic resistance (7).

Medicinal plants have been investigated for their therapeutic value in traditional medical practice and it has been proven that medicinal plants are the natural source of compounds that can be used against many diseases (8). Many plants contain a wide variety of chemicals that have important biological effects on humans (9). Bioactive compounds that develop as a result of secondary metabolic activities of plants, which cannot be consumed as food but have beneficial effects for human health are called 'phytochemicals' (10). These compounds prevent degenerative diseases, act as antiallergenic, anti-inflammatory, antimicrobial, antithrombotic and vasodilator agents (11). The main compounds responsible for the antimicrobial effect in plants are known as phenolics, phenolic acids, quinolones, saponins, flavonoids, tannins, coumarins, terpenoids and alkaloids (12). Phenolic substances constitute the most important groups of natural antioxidants. In addition to their antioxidant activities, they chelate metal ions and inhibit transcription factors that initiate and support tumor development by stimulating detoxifying enzymes (9). In this study, antibacterial and anti-quorum sensing properties of *Citrus medica* L. plant were investigated and some phenolic compounds were determined by HPLC.

2. Methods

2.1. Plant Extraction

The peel of *C. medica* L. was dried in the shade at room temperature away from direct sunlight. It was powdered with the help of a steel blender

(Waring 8011 EB) and 10 g was weighed and 100 mL of solvent (methanol) was added. The solvent-powder mixture was kept in an ultrasonic water bath for half an hour, and the methanol-tree melon mixture taken from the ultrasonic water bath was filtered through coarse filter paper. The plant extract remaining in the flask whose solvent was completely removed in a rotary evaporator (Heidolph Hei-Vap Rotary Evaporator) under vacuum at 40-45°C was weighed and recorded. All of the plant in the flask was extracted with dimethylsulfoxide (DMSO). It was stored in the refrigerator at +4°C.

2.2. High-Performance Liquid Chromatography (HPLC) Analysis

The *C. medica* L. extract's phytochemical composition was assessed using the High-Performance Liquid Chromatography (HPLC) method (13). Table 1 displays the HPLC analytical process.

Table 1. Conditions of chromatography

	Time (min)	A (%)	B (%)
Detector: Photo Diode Array Detector (λ max. 278 nm)	0	93	7
	20	72	28
Autosampler: SIL-10AD vp	28	75	25
System controller: SCL-10A vp	35	70	30
Pump: LC-10AD vp	50	70	30
Degasser: DGU-14a	60	67	33
Column heater: CTO-10 A vp	62	58	42
Column: Agilent Eclipse XDB C-18 (250 mm \times 4.6 mm), 5 μ m	70	50	50
Column temperature: 30 °C	73	30	70
Mobile phases: A: acetic acid–water (3:97 v/v), B: methanol	75	20	80
Flow rate: 0.8 mL/ dak.	80	0	100
Injection volume: 20 μ L	81	93	7

2.3. Minimum Inhibition Concentration (MIC) and Minimum Bactericidal Concentration (MBC) Test

The antibacterial activity of *C. medica* L. was tested on Gram positive (*Bacillus cereus* ATCC 11778, *Enterococcus faecalis* ATCC

29212, *Staphylococcus aureus* ATCC 25923) and Gram negative (*Escherichia coli* ATCC 25922, *Pseudomonas aeruginosa* ATCC 27853, *Pseudomonas aeruginosa* PAO1) bacteria and its quorum sensing effect was tested on *P. aeruginosa* PAO1 and *Chromobacterium violaceum* (CV12472) bacteria. In this method, 96-well microplates were prepared. In the wells containing Mueller Hinton Broth medium, 100 μ L of plant extract was added and two-fold serial dilutions were made respectively. 5 μ L of bacterial suspension adjusted to 0.5 McFarland turbidity was added and the microplates were incubated overnight at 30/37°C. After incubation, the microplates were evaluated and the lowest concentration without growth was determined as the MIC value. Experiments were performed in 3 replicates. MBC test confirmed by point-inoculating MH media from wells for each microorganism tested (14).

2.4. Pyocyanin Inhibition Test

To the LB medium containing *C. medica* L. to be tested for its effect on pyocyanin pigment production, 100 μ L of PAO1 bacterial culture with OD 0.05 at 600 nm was added and incubated at 37°C for 16-18 hours with shaking. Then 5 mL of chloroform was added to PAO1 cultures grown in LB medium and vortexed for 45 seconds. The phase separated from chloroform at the bottom of the bottles was separated into glass tubes as 2 mL. Then 1 mL of 0.2 M HCl-water was added to the glass tubes and vortexed for 45 seconds and the pink phase formed at the top of the tubes was read at OD 520 nm and recorded. The experiment was performed in 3 replicates (15).

2.5. Biofilm Inhibition Test

Luria Bertani Broth (LBB) medium, 20 μ L *C. medica* L. and 5 μ L PAO1 bacteria equivalent to 0.5 McFarland turbidity were added to 96 microplates and the microplate was incubated for 48 hours. After 48 hours, the contents were poured out and washed three times with distilled water, 0.1% crystal violet was added to the wells as 200 μ L and waited for 30 minutes. After waiting, the crystal violet was poured and washed three times

with distilled water. 200 μL of 95% EtOH was added to each well and waited for another 15 min. The results were read at OD 570 nm, compared with the control and recorded. The experiment was performed in 3 replicates (16).

2.6. Violacein (*C. violaceum* 12472) Pigment Inhibition Test

Overnight culture (10 μL) of *C. violaceum* (adjusted to 0.4 OD at 600 nm) was added to sterile microplates containing 200 μL . Microplates containing CV12472 and *C. medica* L. as positive control were incubated at 30 $^{\circ}\text{C}$ for 24 h and observed for the decrease in violacein pigment production. Absorbance was read at 585 nm. The experiments were performed in 3 replicates (17).

2.7. Statistical Analysis

This study was designed according to the “randomized plots experimental design” and three replicates were used in each treatment. The data were subjected to analysis of variance (ANOVA) with JUMP statistical package program and the differences between treatments were evaluated with LSD multiple comparison test.

3. Results

3.1. HPLC Results

The presence of protocatechic acid, catechin, epicatechin, sinapinic acid, benzoic acid, rutin, hesperidin, and cinnamic acid is demonstrated by the HPLC chromatogram of the methanolic extract of *C. medica* L. A sample chromatogram is displayed in Fig 1.

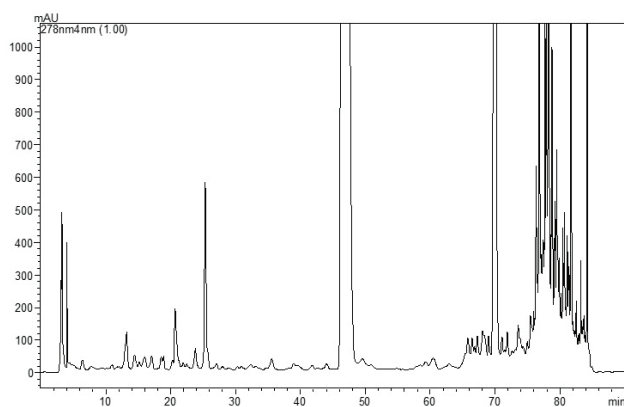


Figure 1. HPLC chromatogram for the main phenolic compounds identified in the methanolic extract of *C. medica* L.

During the chromatogram, the common spectrum containing the peak maximums of each analyte was studied at 278 nm. The highest concentration was found in benzoic acid as 41.9 $\mu\text{g}/\text{mL}$, which was followed by sinapinic acid as 7.6 $\mu\text{g}/\text{mL}$, cinnamic acid as 7.0 $\mu\text{g}/\text{mL}$ (Table 2). Also, catechin as 6.3 $\mu\text{g}/\text{mL}$, hesperidin as 4.7 $\mu\text{g}/\text{mL}$, rutin as 3.5 $\mu\text{g}/\text{mL}$, epicatechin as 1.9 $\mu\text{g}/\text{mL}$, protocatechic acid as 0.5 $\mu\text{g}/\text{mL}$ phytochemicals.

Table 2. Concentrations of the primary phenolic components found in *C. medica* L.'s methanolic extract.

Phytochemicals	Concentrations ($\mu\text{g}/\text{mL}$)	Retention time (min)
Protocatechic acid	0.5	9.0
Catechin	6.3	12.70
Epicatechin	1.9	19.7
Sinapinic acid	7.6	31.3
Benzoic acid	41.9	36.9
Rutin	3.5	46.1
Hesperidin	4.7	52.6
Cinnamic acid	7.0	68.3

3.2. MIC and MBC Test Results

The minimum inhibition concentration of *C. medica* L. was studied on Gram positive and Gram negative bacteria and the values are given in Table 3. According to the table, the best antibacterial effect of *C. medica* L. was observed on *C. violaceum* 12472. The weakest antibacterial effect was observed on *E. coli* and *S. aureus* bacteria.

Table 3. MIC and MBC results of *C. medica* L. peel extract

Microorganisms	MIC (mg/mL)	MBC (mg/mL)
<i>E. coli</i> ATCC 25922	60	121
<i>S. aureus</i> ATCC 25923	60	121
<i>P. aeruginosa</i> PAO1	30	60
<i>P. aeruginosa</i> ATCC 27853	30	60
<i>B. cereus</i> ATCC 11778	30	60
<i>C. violaceum</i> CV 12472	15	30

3.3. Pyocyanin Inhibition Test

Many *P. aeruginosa* strains are soluble bacteria, giving the colonies a blue-green color pyocyanin, a phenazine-derived pigment has the ability to produce *P. aeruginosa* low molecular weight produced by pyocyanin molecule, which has

important is one of the pathogenicity factors. Respiratory pathways interrupted ciliary activity and oxidative and is responsible for neutrophil-associated tissue damage (18,19). Pyocyanin production test proved that *C. medica* L. inhibited pyocyanin pigment production in PAO1 by 20%. Although an average inhibition was observed, it was statistically significant ($p < 0.01$) (Fig 2).

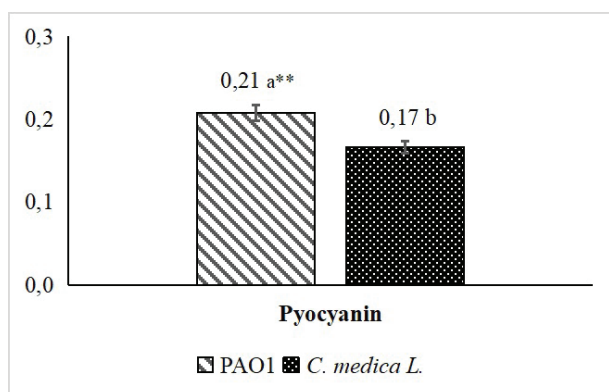


Figure 2. Inhibition effect of *C. medica* L. on pyocyanin production. **The difference between the means shown with different letters is statistically significant ($p < 0.01$).

3.4. Biofilm Inhibition Test

According to test result of biofilm formation on PAO1, it was observed that *C. medica* L. had a high inhibitory effect of 88% on biofilm formation (Fig 3).

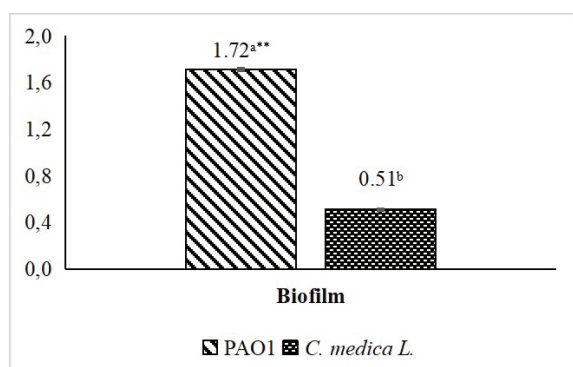


Figure 3. Inhibition effect of *C. medica* L. on biofilm formation. **The difference between the means shown with different letters is statistically significant ($p < 0.01$).

3.5. Violacein Inhibition Test

In *C. violaceum*, the QS system is responsible for violacein (purple) pigment formation. In this study, *C. medica* L. inhibited violacein pigment formation by 32% (Fig 4).

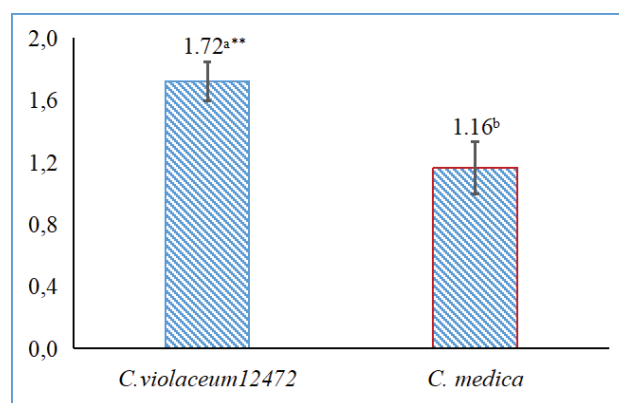


Figure 4. Inhibition effect of *C. medica* L. on violacein pigment formation. **The difference between the means shown with different letters is statistically significant ($p < 0.01$).

4. Discussion

The need for novel antimicrobial agents is growing because bacteria can become resistant to existing medications. Medicinal plants are abundant in bioactive substances that have antibacterial properties. Since *C. medica* L. contains a large concentration of phytochemicals with antimicrobial characteristics, like citral, linalool, and limonene its antimicrobial properties are unquestionably the best studied of its various biological properties (20-22). The *C. medica* L. is the oldest wild product of the citrus family known to possess various pharmacological and nutraceutical properties. The presence of phytochemicals in the peel and leaves shows antioxidant effects that have a protective effect against many diseases such as diabetes, cancer, hypercholesterolemia and other chronic diseases caused by various oxidative stresses (23). In this study, antibacterial and quorum sensing properties of *C. medica* L. were investigated and as a result of the experiments, the presence of antibacterial effect of *C. medica* L. on various bacteria was demonstrated and MIC-MBC concentration were determined. While it was found to have a similar MIC value on Gram positive and Gram negative bacteria, the lowest MIC and MBC value was found on *C. violaceum* with a concentration of 30/60 mg/mL. In a study an ethanol extract from the exocarp of *C. medica* var. *sarcodactylis* was effective against *B. cereus* (MIC 2.5 mg/mL) than *E. coli* (MIC 10 mg/mL). The exocarp extract's increased antibacterial action could be explained

by its higher coumarin concentration (24). The main component of *C. medica* L. used in this study was found to be benzoic acid after hplc test and it has been reported in previous studies that the antimicrobial activity of benzoic acid is primarily against yeasts and molds (25).

The antibacterial properties of extracts from the roots, leaves, and bark of the *C. medica* species grown in Uttarakhand, India's Kumaun region were evaluated on a number of bacterial strains. The root and juice extracts exhibited the greatest activity, with inhibition zones of 19 mm and 17 mm, respectively. These values were even greater than those of the conventional medication, chloramphenicol, which has an inhibition zone of 14 mm (26). Sharma et al., on the other hand, reported that a *C. medica* L. juice extract did not affect the development of *B. subtilis*, *S. aureus*, *E. coli* or *K. pneumoniae* (27).

Plant contents may show annual changes depending on the region where they grow, rainfall rate and different climatic conditions (28). In this regard, Sun et al. found through a meta-analysis that the amounts of phenolic compounds in aromatic and medicinal plants rise in response to yearly rainfall declines and temperature rises (29).

The fact that the QS system is effective in the infection process has resulted in an increasing number of studies on the inhibition of the system. For this purpose, many natural and synthetic molecules have been the subject of studies and especially plants have been the focus of studies due to their rich content. In this study, one of the subjects investigated was the inhibition of violacein pigment in *C. violaceum* and as a result of the tests performed a statistically significant 32% inhibition of *C. medica* L. was observed. In the literature review, no studies on pigment inhibition in *C. violaceum* with *C. medica* species were found. Additionally in this study, *C. medica*, whose quorum sensing activity was investigated and was found to inhibit the production of pyocyanin pigment production in *P.aeruginosa* PAO1 strain by 20%, while it was found to have a high inhibition effect on biofilm formation with a high rate of 88%. Biofilm consists of groups of bacteria attached to surfaces and encapsulated in a hydrated

polymeric matrix. *P. aeruginosa* biofilms cause persistent infections in individuals with major health problems (30). Therefore, their treatment is of great importance and alternative approaches to antibiotics are gaining attention day by day. *Campylobacter jejuni*'s antibacterial efficacy against *C. medica* L. by products (peel, seeds) was evaluated by Castillo et al. The extract decreased the production of biofilms (60–75%) and swarm motility (35–40%) (31). In our results biofilm inhibition rate was 88% and the difference between the studies is due to differences in the region where the material grows, the concentrations studied and the types of microorganism.

5. Conclusion

In recent years, the use of plant-derived extracts has received increasing attention due to concerns over possible adverse health effects caused by the use of traditional medicines. In particular, antibiotic resistance has become a global problem and new approaches to combat it have become mandatory. In this study, some of the constituents of *C. medica* L. were investigated and their effects on bacteria were also examined. In conclusion, based on the current literature review and this study, it is possible to say that *C. medica* L. can be considered as a good candidate for the treatment of various pathologies related to microbial infection and prevention of biofilm formation. However, further studies are needed to maximize the potential of *C. medica* L. on human health.

Conflicts of interest: There are no conflicts of interest among the authors.

References

1. Sancak B. Staphylococcus aureus ve antibiyotik direnci. Mikrobiyol Bul. 2011;45(3): 565-576.
2. Luís Â, Duarte A, Gominho J, Domingues F, Duarte AP. Chemical composition, antioxidant, antibacterial and anti-quorum sensing activities of Eucalyptus globulus and Eucalyptus radiata essential oils. Ind Crops and Prod. 2016;79:274-282. doi:10.1016/j.indcrop.2015.10.055
3. Isbilir SS, Sagioglu A. An assessment of in vitro antioxidant activities of different extracts from

- Papaver rhoeas L. leaves. *International Journal of Food Properties*. 2012; 15(6):1300-1308. doi:10.1080/10942912.2010.520542
4. Çepni E, Gürel F. Bitkilerden Elde Edilen Anti-Quorum Sensing Bileşikleri Ve Yeni İlaç Geliştirmedeki Potansiyelleri. *Türk Mikrobiyoloji Cemiyeti Dergisi*. 2011;41(4): 131-138. doi:10.5222/TMCD.2011.131
 5. Tinaz GB. Quorum sensing in gram negative bacteria. *Turk J Biol*. 2003;27(2): 85-93.
 6. Whitehead NA, Barnard AM, Slater H, Simpson NJ, Salmond GP. Quorum-sensing in Gram-negative bacteria. *FEMS Microbiol Rev*. 2001;25(4):365-404. doi: 10.1111/j.1574-6976.2001.tb00583.x
 7. Chong YM, Yin WF, Ho CY, Mustafa MR, Hadi AHA, Awang K, Chan KG. Malabaricone C from *Myristica cinnamomea* exhibits anti-quorum sensing activity. *J. Nat. Prod*. 2011;74(10):2261-2264. doi:10.1021/np100872k
 8. Vital PG, Lasco JRN, Demigillo JM, Rivera WL. Antimicrobial activity, cytotoxicity and phytochemical screening of *Ficus septica* Burm and *Sterculia foetida* L. leaf extracts. *J. Med. Plant Res*. 2010;4: 58-63. doi:10.5897/JMPPR09.400
 9. Faydaoğlu E, Sürücüoğlu M. Tıbbi ve aromatik bitkilerin antimikrobiyal, antioksidan aktiviteleri ve kullanım olanakları. *EÜFBED - Fen Bilimleri Enstitüsü Dergisi*. 2013; 6(2): 233-265.
 10. Visioli F, Galli C, Plasmati E, Viappiani S, Hernandez A, Colombo C, Sala A. Olive phenol hydroxytyrosol prevents passive smoking-induced oxidative stress. *Circulation*. 2000;102: 2169-2171. doi:10.1161/01.cir.102.18.2169
 11. Halliwell B. Dietary polyphenols: good, bad, or indifferent for your health. *Cardiovasc. Res*. 2007;73:341-347. doi:10.1016/j.cardiores.2006.10.004
 12. Gyawali R, Ibrahim SA. Natural products as antimicrobial agents. *Food Control*. 2014;46: 412-429. doi:10.1016/j.foodcont.2014.05.047
 13. Caponio F, Gomes T, Pasqualone A. Phenolic compounds in virgin olive oils: influence of the degree of olive ripeness on organoleptic characteristics and shelf-life. *Eur Food Res Technol*. 2001; 212: 329-333. doi:10.1007/s002170000268
 14. Noumi E, Ahmad I, Bouali N, Patel H, Ghannay S, Alrashidi AA, Abdulhakeem MA, Patel M, Ceylan O, Badraoui R, Elkahoui S, Hedia F, Sdouga D, Abaza C, Smach MA. *Thymus musilii* Velen. Methanolic extract: In vitro and in silico screening of its antimicrobial, antioxidant, anti-quorum sensing, antibiofilm, and anticancer activities. *Life*. 2023; 13(1):62. doi:10.3390/life13010062
 15. Essar DW, Eberly L, Hadero A, Crawford I. Identification and characterization of genes for a second anthranilate synthase in *P. aeruginosa*: interchangeability of the two anthranilate synthases and evolutionary implications. *J. Bacteriol*. 1990;172:884-900. doi:10.1128/jb.172.2.884-900.1990
 16. O'Toole GA. Microtiter dish biofilm formation assay. *J Vis Exp*. 2011;(47):2437. doi:10.3791/2437.
 17. Ngenge AT, Kucukaydin S, Ceylan O, Duru ME. Evaluation of enzyme inhibition and anti-quorum sensing potentials of *Melaleuca alternifolia* and *Citrus sinensis* essential oils. *Nat. Prod. Commun*. 2021;16(9). doi:10.1177/1934578X211044565
 18. Fuqua C, Parsek MR, Greenberg EP. Regulation of gene expression by cell to-cell communication: acyl-homoserine lactone quorum sensing. *Annu Rev Genet*. 2001; 35:439-468. doi:10.1146/annurev.genet.35.102401.090913
 19. Önem E, Sarisu HC. Bazı uçucu yağların *P. aeruginosa* PAO1 virülansında etkinliği. *Tıp Fakültesi Klinikleri Dergisi*. 2021; 4(2): 75-82. doi:10.17932/IAU.TFK.2018.008/tfk_v04i2004
 20. Benedetto N, Carlucci V, Faraone I, Lela L, Ponticelli M, Russo D, Mangieri C, Tzvetkov NT, Milella L. An Insight into *Citrus medica* Linn. A Systematic Review on phytochemical profile and biological activities. *Plants (Basel)*. 2023; (12):2267. doi:10.3390/plants12122267.
 21. Punitha V, Vijayakumar S, Nilavukkarasi M, Vidhya E, Praseetha P. Fruit peels that unlock curative potential: Determination of biomedical application and bioactive compounds. *S. Afr. J. Bot*. 2022;150:1051-1060. doi:10.1016/j.

- sajb.2022.09.022
- 22.** Nagy MM, Al-Mahdy DA, Abd El Aziz OM, Kandil AM, Tantawy MA, El Alfy TS. Chemical composition and antiviral activity of essential oils from Citrus reshni hort. ex Tanaka (Cleopatra mandarin) cultivated in Egypt. J. Essent. Oil-Bear. Plants. 2018; 21:264-272. doi:10.1080/0972060X.2018.1436986.
- 23.** Chhikara N, Kour R, Jaglan S, Gupta P, Gat Y, Panghal A. Citrus medica: nutritional, phytochemical composition and health benefits - a review. Food Funct. 2018 ;9(4):1978-1992. doi: 10.1039/c7fo02035j
- 24.** Sahoo CR, Sahoo J, Mahapatra M, Lenka D, Sahu PK, Dehury B, Padhy RN, Paidasetty SK. Coumarin derivatives as promising antibacterial agent(s). Arab.J. Chem. 2021;14:102922. doi:10.1016/j.arabjc.2020.102922
- 25.** Zeece M. Introduction to the Chemistry of Food. Academic Press; 2020.
- 26.** Sah AN, Juyal V, Melkani AB. Antimicrobial activity of six different parts of the plant Citrus medica Linn. Pharmacogn. J. 2011;3:80-83. doi:10.5530/pj.2011.21.15
- 27.** Sharma R, Verma S, Rana S, Rana A. Rapid screening and quantification of major organic acids in citrus fruits and their bioactivity studies. J. Food Sci. Technol. 2018; 55:1339-1349. doi:10.1007/s13197-018-3045-x
- 28.** Pérez-Ochoa ML, Vera-Guzmán AM, Mondragón-Chaparro DM, Sandoval-Torres S, Carrillo-Rodríguez JC, Mayek-Pérez N, Chávez-Servia JL. Effects of annual growth conditions on phenolic compounds and antioxidant activity in the roots of Eryngium montanum. Plants. 2023;3:12(18):3192. doi:10.3390/plants12183192
- 29.** Sun Y, Alseekh S, Fernie AR. Plant secondary metabolic responses to global climate change: A meta-analysis in medicinal and aromatic plants. Glob. Change Biol. 2023;29, 477-504. doi:10.1111/gcb.16484
- 30.** Banin E, Vasil ML, Greenberg EP. Iron and Pseudomonas aeruginosa biofilm formation. PNAS. 2005;102;31:11076-11081. doi:10.1073/PNAS.0504266102
- 31.** Castillo S, Heredia N, Arechiga-Carvajal E, García S. Citrus Extracts as inhibitors of quorum sensing, biofilm formation and motility of Campylobacter jejuni. Food Biotechnol. 2014;28(2), 106-122. doi: 10.1080/08905436.2014.895947

Cite this article: Gunes HH, Onem E. Phytochemical Profile and Antibacterial-AntiQuorum Sensing Properties of *Citrus medica* L. Pharmedicine J. 2024;1(3); 102-109. DOI: 10.62482/pmj.14



Original Article

Amino Acid Supported Conductive Nanocomposite for Developing Flexible Electrode Material for Energy Storage

Sinem Ortabay¹, Melisa Ogretici¹, Kibar Aras², Elif Caliskan Salih³

¹Istanbul University-Cerrahpaşa, Faculty of Engineering, Department of Chemistry, Istanbul, Türkiye

²Ataturk University, Faculty of Science, Department of Chemistry, Erzurum, Türkiye

³Marmara University, Faculty of Pharmacy, Department of Basic Pharmacy Sciences, İstanbul, Türkiye

 Corresponding Author: Sinem Ortabay E-mail ortabay@iuc.edu.tr)

Received: 2024.10.17; Revised: 2024.10.22; Accepted: 2024.10.24

Abstract

Introduction: This study focused on synthesizing biocompatible, flexible and wearable electrode materials for energy storage applications. The unique zwitterionic structure of L-proline provides numerous interesting properties to the nanocomposite such as high ionic interactions through the various ion migration channels, and strong hydration characteristics. These features are key to the high performance of energy deposition systems.

Methods: Binary nanocomposites containing L-proline (Pro) amino acid and polypyrrole (Ppy) were produced on rGO modified carbon textile (rGO-CC) to develop electroactive materials. Two-step hydrothermal method was used to produce flexible electrodes. DRIFT spectroscopy and AFM analysis were performed to clarify the structural and the morphological characterization. Electrochemical behavior was evaluated utilizing CV, GCD and EIS methods.

Results: ProPpy@rGO-CC electrode materials exhibit high electrochemical performances in aqueous electrolytes (0.1 M NaCl). The prepared electrode shows high specific capacitance of 500.4 Fg⁻¹ (at 25 mVs⁻¹) at the ambient conditions. Additionally, after 5,000 charge/discharge cycles the specific capacitance retains a high level of 95% confirming the good cycle stability. The energy and the power densities were found to be 278 Wh kg⁻¹ and 12.5 kW kg⁻¹, respectively.

Conclusion: The results indicate that the ProPpy@rGO-CC electrode is a promising candidate for next-generation high-performance energy deposition systems. The unique structural features of L-proline contribute to the formation of a large number of electroactive sites and short diffusion pathways.

Keywords: Energy storage, amino acids, reduced graphene oxide, polypyrrole, supercapacitor

1. Introduction

Batteries and supercapacitors are critical components in modern renewable energy storage technologies. Particularly,

supercapacitors have higher power density, long cycle life, and rapid charge-discharge characteristics when compared to the batteries. On one hand, recent advancements in supercapacitor technology have led to the

development of new materials and designs that improve their energy density, and making them more competitive with batteries. On the other hand, integrating supercapacitors with biological systems enhances bioenergy applications' performance. For example, wearable devices that harvest energy from human biofluids or movements can benefit from the rapid energy storage capabilities of supercapacitors. These devices can be utilized as biofuel cells to convert the biochemical energy into the electrical energy, which is then stored in supercapacitors for later use (1,2). This synergy not only enhances the efficiency of energy harvesting systems but also enables the development of self-powered wearable electronics (3).

Very recently, biological samples such as enzymes, amino acids, bacterial medium, etc. are extensively used as electrolyte materials or electrode active materials during the fabrication process of supercapacitor devices (4). Among biological systems, amino acid-based supercapacitors represent a promising area of research in energy storage technology. The utilization of amino acids as components in supercapacitors leverages their unique chemical properties, such as the presence of functional groups that can facilitate charge storage and enhance electrochemical performance. This approach not only contributes to the development of more efficient energy storage devices but also aligns with the growing demand for sustainable and biodegradable materials.

One of the primary advantages of using amino acids in supercapacitors is their ability to participate in protonation and deprotonation processes, which are essential for charge storage. Amino acids contain charged side chains, such as lysine, arginine, and glutamic acid that can undergo these reversible reactions, thus contributing to the capacitive charge storage mechanism. This characteristic is particularly beneficial for the design of ultrafast supercapacitors, where rapid charge and discharge cycles are crucial (5). Research has demonstrated that amino acids can serve as effective doping agents in the synthesis of carbon-based materials for supercapacitors. For instance, nitrogen-doped graphene hydrogels have been synthesized using amino acids, which not only improve the

conductivity of the material but also enhance its electrochemical performance. The hydrothermal synthesis process allows the integration of amino acids into the graphene structure, resulting in materials with high surface areas and improved charge storage capabilities (6). Furthermore, amino acids can act as precursors for the production of nitrogen-doped carbon materials, which have shown significant promise in enhancing the performance of supercapacitors (7,8).

The development of amino acid ionic liquids (AAILs) has also opened new avenues for supercapacitor technology. AAILs exhibit favorable electrochemical properties, including high ionic conductivity and stability, making them suitable electrolytes for supercapacitors (9,10). Studies have shown that supercapacitors utilizing AAILs can achieve capacitance values comparable to those of conventional ionic liquid-based systems, thus demonstrating their viability as a sustainable alternative (9).

Moreover, the use of amino acids in the synthesis of metal-organic frameworks (MOFs) has been explored for their application in asymmetric supercapacitors. Amino-functionalized MOFs can provide high specific capacitance and serve as binder-free electrodes which simplifies the fabrication process and enhances the overall performance of the supercapacitor (11). This approach highlights the versatility of amino acids in creating advanced materials for energy storage applications. The unique properties of amino acids, such as their ability to participate in charge storage mechanisms and their vital role as precursors for advanced materials, make them as valuable components in the next generation of energy deposition systems. Ongoing research in this area is likely to give innovative approaches that meet both performance and environmental concerns in energy storage applications.

In the present study, an active electrode was synthesized using L-proline-derived conductive polymer on flexible textile substrates deposited with reduced graphene oxide (rGO). Hydrothermal method was applied to the synthesis of the active electrode composed of L-proline, and a

polypyrrole conductive polymer. The electrode obtained was evaluated electrochemically using cyclic voltammetry (CV), galvanostatic charge-discharge (GCD), and electrochemical impedance spectroscopy (EIS). The characterization of the electrode materials was performed diffuse reflectance infrared Fourier transform spectroscopy (DRIFT), Raman spectroscopy and atomic force microscopy (AFM) techniques.

2. Methods

2.1. Apparatus

Gamry 1010E Potentiostat/Galvanostat system (Gamry Instruments, Inc., Warminster, PA, USA) was used for all voltammetric measurements. Conventional three-electrode and two electrode systems were utilized in the investigation of electrode and supercapacitor performances, respectively. ProPpy@rGO-CC electrode (1x3 cm²) served as the working electrode, a Ag/AgCl (3M KCl) electrode and Pt plate (0.5 cm²) served as the reference and the counter electrode, respectively. The data was analyzed with an Echem Analyst 2 software interfaced with a computer (version 7.8.2). Carbon cloths (CC) were used as the flexible current collectors to produce ProPpy@rGO-CC electrode. The technical and mechanical properties of CC are given in Table 1.

Table 1. The technical and the mechanical properties of carbon cloth

The Technical and The Mechanical Properties of Carbon Cloth			
Weave	2/2 twill	Tensile Modulus	240 GPa
Weight	200 gm ⁻²	Filament Diameter	7 mm
Density	1.76 gcm ⁻³	Elongation	1.7 %
Dry fabric thickness	0.2 mm	Fiber	Carbon 3K
Tensile strength	3950 MPa	Specific electrical resistance	1.6 x 10 ⁻³ Wcm

Deionized water (DI) obtained from a Nüve water distillation system which was used throughout the experiments.

The electrochemical impedance spectroscopy (EIS) measurements were performed in the frequency range between 0.1 Hz and 100 kHz with

an amplitude of superimposed alternative current (AC) signal of 10.0 mV at the open circuit potential (OCP).

The height asymmetries and nanostructural properties of the electrode surface were clarified by AFM, which was produced by Nanomagetics-Instrument. It was operated in dynamic mode using aluminum coated silicon tips (PPP-NCLR, Nanosensors, Switzerland). The technical properties of the AFM tips were given in the following Table 2.

Table 2. The technical properties of the AFM tips

Property	Nominal Value	Specified Range
Resonance Frequency [kHz]	190	146 - 236
Force Constant [N/m]	48	21 - 98
Length [μm]	225	215 - 235
Mean Width [μm]	38	30 - 45
Thickness [μm]	7	6 - 8

Samples were recorded with the scanning rate of 5 μm⁻¹ and 256 × 256 pixels resolution to obtain a view of 5 × 5 μm² area. The AFM images were evaluated using the “NMI Viewer 2.0.7. Image Analyzer” software. Diffuse Reflectance Infrared Fourier Transform Spectroscopy (DRIFT) techniques were applied for the chemical characterization of active electrode materials. The DRIFT spectra were obtained using Bruker-Alpha T model spectrophotometer. Mass ratio of active electrode material to KBr was kept constant at 1/150 (w/w). All electrochemical experiments were performed at room temperature (25 ± 2 °C, 54% humidity)

2.2. Preparation of ProPpy@rGO-CC electrodes

The modified Hummer’s method was adopted to produce graphene oxide (GO). Hence, 0.5 g of graphite powder and 3 g of KMnO₄ were mixed in a mortar and pestle. H₂SO₄ and H₃PO₄ mixture in the ratio of 9:1 was added to the powder mixture with continuous magnetic stirring. The greenish black solution was obtained. Then, the heating process was applied to the solution (60 °C - 24 h) until the color of solution turned to brown color. The dropwise addition of H₂O₂ (30%) was carried out in an ice bath. After the yellow color was seen,

the product was washed thoroughly with DI water and ethanol followed by the drying at 55 °C. Then, hydrothermal synthesis was used to fabricate rGO-CC. Firstly, suspension of 50 mg of as-synthesized GO in 25 mL of ethylene glycol were prepared by sonication during 30 min. The resulted colloidal solution turned to brown color. The mixture was poured into the Teflon-lined autoclave for 12 hours keeping at 150 °C. At the same time, the textile substrate in the dimension 3x1 cm² was placed in to the autoclave. After the hydrothermal process the rGO-CC electrode washed thoroughly with acetone and DI water. Finally, it was dried in an oven at 55 °C overnight. L-proline solution in ethanol, pyrrole, and (NH₄)₂S₂O₈ were mixed in an ultrasonic bath. The mix solution and the rGO-CC was transferred to the sealed Teflon lined autoclave and was placed at 120 °C for 12 hours in a furnace. The resulting electrode was cleaned and dried applying the same procedure as mentioned above. The electrode obtained was named as ProPpy@rGO-CC.

3. Result and Discussion

3.1. Structural Characterizations

Fig 1 shows the Raman spectra of GO powder and rGO films hydrothermally deposited on the textile substrate. The typical prominent bands observed at ~1600 cm⁻¹ (G band) and at ~1345 cm⁻¹ (D band), caused by E_{2g} mode (sp² carbon) in graphene and breathing mode of aromatic moieties were clarified (12). Additionally, the weak broad bands located

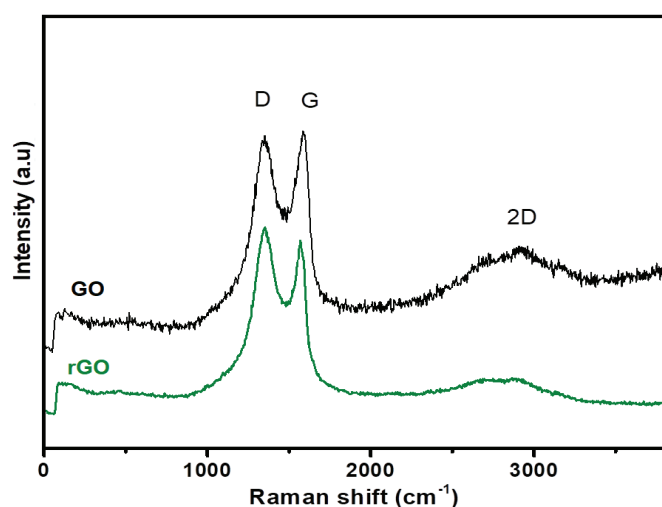


Figure 1. Raman spectra of GO powder and rGO film deposited onto CC substrate

at about 2690, 2940 and 3180 cm⁻¹ also identified from the spectra (2D band). The intensity ratio of D bands and G bands (I_D/I_G) gives the critical information about defect regions of carbon lattice. The ratio of I_D/I_G increases in the presence of rGO in the structure due to the transformation and enhanced disorder following chemical reduction (13). This trend corresponds to the findings obtained from the present study. The I_D/I_G ratios are found as 0.96 and 1.13 for GO and rGO, respectively.

Furthermore, the 2D band, also provides an important aspect regarding the number of graphene layers and the electronic structure of the material. In rGO, the 2D band generally exhibits a shift towards lower wavenumbers compared to GO, which can be attributed to changes in the electronic environment and the reduction in the number of layers (14,15). In this study, the 2D bands in rGO located about 20 cm⁻¹ wavenumbers less when compared to those of GO bands confirming the formation of rGO.

Fig 2 presents the DRIFT spectrum of ProPpy@rGO-CC electrode. In the spectrum the peaks observed at 822 and 1030 cm⁻¹ were ascribed to PPy structure, whereas the peaks at 3326, 2935, 1727, 1517, 1393, 1251, and 1098 cm⁻¹ are assigned to N-H, C-H (sp³), C=O, C-N, C=C (backbone stretching), N-O, C-O, and C-C stretching, respectively, describing the characteristics of PPy and L-proline (16). The peak observed at 1517 cm⁻¹ is attributed to the carboxyl group of GO.

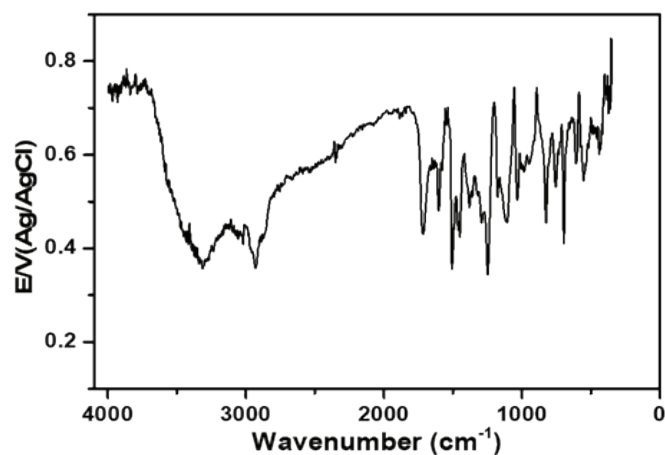


Figure 2. DRIFT spectrum of ProPpy@rGO film on textile substrate

Polypyrrole exhibits significant interactions with amino acids, which can be leveraged in various

applications, including biosensors, energy and drug delivery systems due to the unique chemical structure of both polypyrrole and the amino acid moieties. In this study, one of the primary mechanisms of interaction between polypyrrole and L-proline is electrostatic attraction. Oxidized polypyrrole, which carries anionic charges, enhances its affinity for L-proline allowing for selective binding based on charge interactions (17). Additionally, it was proposed that L-proline can interact with polypyrrole through multiple bonding mechanisms involving electrostatic, hydrogen bonding, and covalent interactions. These interactions not only influence the binding affinity of amino acids to polypyrrole but also enhance the functional properties of the

polymer for various applications in materials, science and biochemistry (18,19). The role of amino acids in modulating the properties of polypyrrole is also significant. For example, the incorporation of amino acids can alter the electrochemical properties of polypyrrole, enhancing its conductivity and stability, which is crucial for applications in energy and biosensing (17). Furthermore, π - π interactions and hydrogen bonding between the rGO layers and aromatic rings of PP and L-proline also play an important role in the formation of hybrid nanocomposites (20). The proposed interaction mechanism is shown in the following illustration (Fig 3).

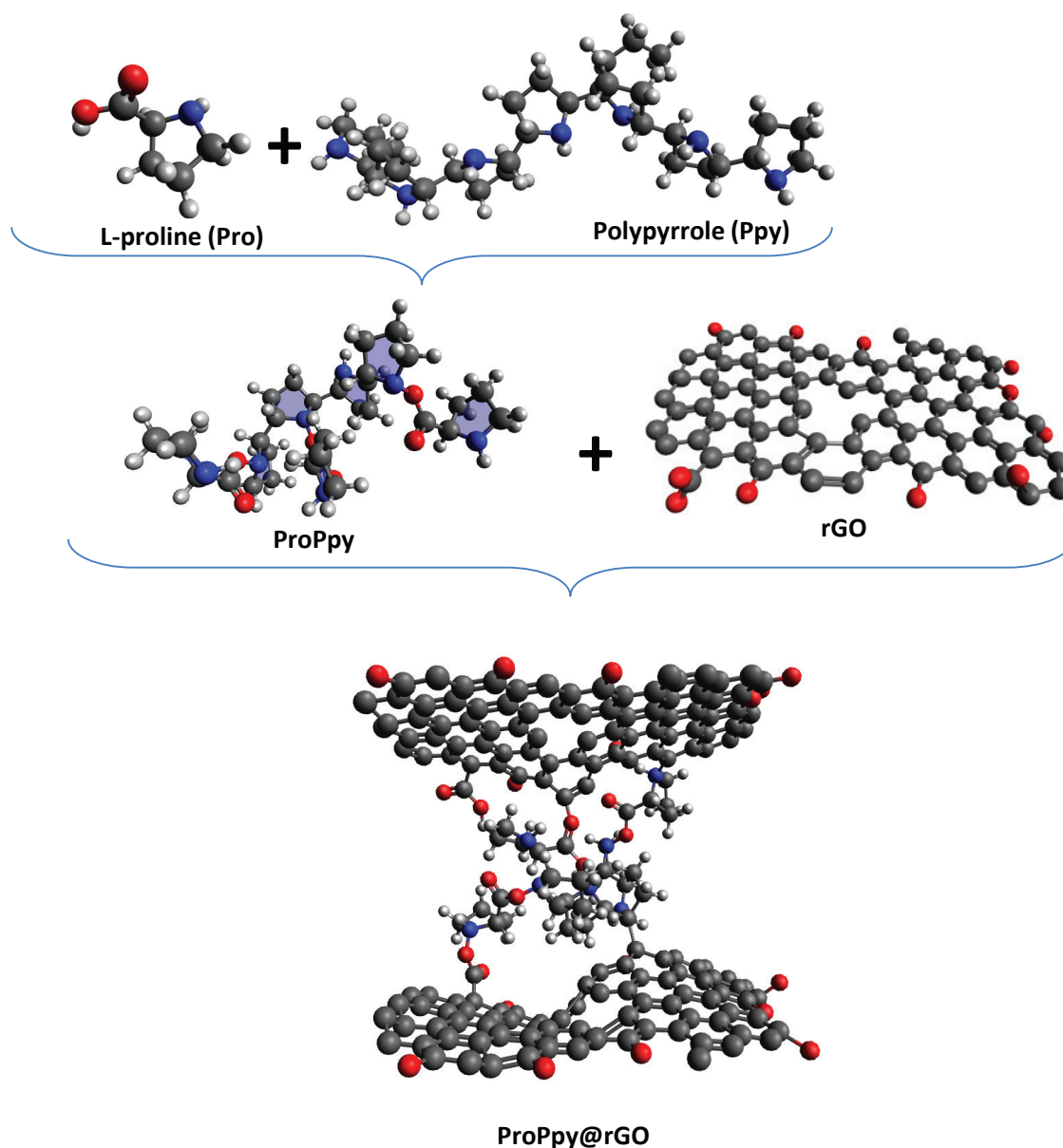


Figure 3. Schematic illustration of reaction mechanisms of ProPpy@rGO deposited on textile substrate.

3.2. Morphological Characterizations

The morphological characterization of the ProPpy@rGO-CC electrode was investigated via the AFM technique. The phase images provide insights into the mechanical properties and structural variations within the composite materials, which are crucial for understanding their performance in various applications. Phase separation can lead to distinct regions within the composite, affecting its electrical and mechanical properties. Moreover, the morphology of polypyrrole composites can be influenced by the presence of L-Proline and rGO. It is well known that phase separation can significantly alter the electrical conductivity of the materials (21,22). Fig 4 exhibits the detailed phase profiles of the ProPpy@rGO-CC electrode. According to Fig 4, the film dimensions investigated are approximately $5 \times 5 \mu\text{m}^2$.

Depending on their unique properties, such as surface energy and modulus, the bright regions show the hard segments, while the dark areas indicate the

soft segments of the electrode material (23,24). As shown in Fig 4a and 4c, the polymeric structures, L-proline, and rGO are evenly distributed in the matrix. The histogram profile revealed positive phase shifts relative to the 90° phase shift observed at resonance, implying that a repulsive force is effective between the tip and the sample surface for investigated segments. Additionally, the cross-section profile obtained from the linear line on the 2D phase image shows the phase distribution fluctuated between $5\text{-}20^\circ$ for different segments.

3.3. Electrochemical Characterization of ProPpy@rGO-CC Electrodes

Electrochemical performance of ProPpy@rGO-CC electrode was evaluated using cyclic voltammetry (CV), galvanostatic charge-discharge (GCD) and electrochemical impedance spectroscopy (EIS) techniques. CV analysis was performed at a potential window of $-1.0 \text{ V} - 1.0 \text{ V}$ with various scan rates from 0.005 Vs^{-1} to 0.5 Vs^{-1} . 0.1 M NaCl aqueous solution was served as an electrolyte to

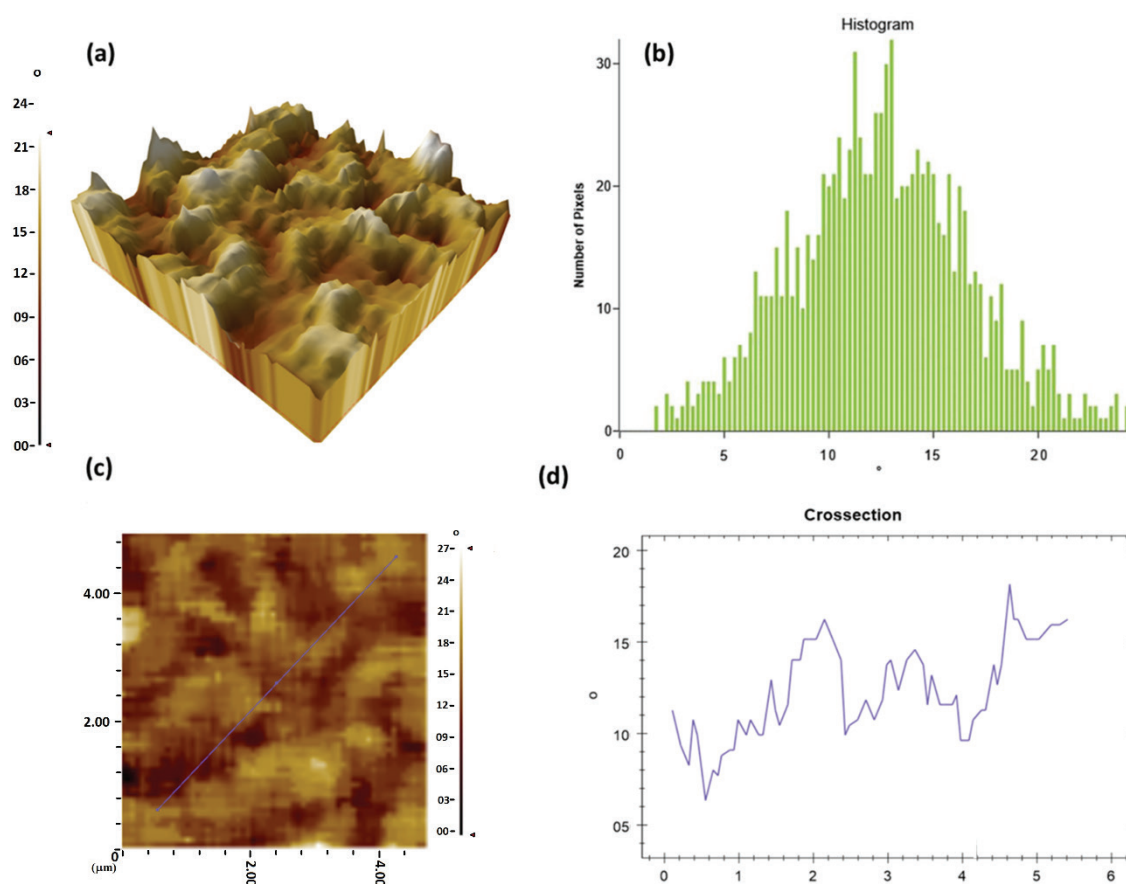


Figure 4. AFM phase images of the ProPpy@rGO-CC electrode, **a)** 3D view, **b)** the phase distribution histogram curve, **c)** 2D view and crosssectional line, **d)** the phase changes through the crosssectional line.

provide biocompatible medium for biological applications. The specific capacitance C (Fcm^{-2}) of the film electrode was determined by means of cyclic voltammetry (CV) according to the following equation.

$$C = \int \frac{Idv}{A\theta(\Delta V)} \quad (1)$$

Where ΔV is the potential window, $\Delta V = (V_{\text{final}} - V_{\text{initial}})$, A is the active surface area of the electrode (cm^2), I is the responsive current (A), and v is the scan rate (Vs^{-1}).

The CV curves of ProPpy@rGO-CC electrode shows a faradic nature as shown in Fig 5a. At relatively low scan rate (25 mVs^{-1}) well-defined

reversible redox peaks were observed which indicate that a pseudo-capacitive behavior based on a redox (faradaic) mechanism is effective. Both the increase in maximum peak currents and the shift of the oxidation/reduction peak potentials towards higher and lower overpotentials further indicate that the prepared electrode possesses desirable electrochemical properties such as enhanced interaction at electrode/electrolyte surface, high surface area and good electrical conductivity (25). The peak separations as a function of scan rates is given in Fig 5a inset.

For further characterization, galvanostatic charge discharge curves were measured at different current densities with potentials between $-1.0 \text{ V} - 1.0 \text{ V}$ (Fig 5b). To observe the complete reaction between the electrode and the electrolyte interface, relatively

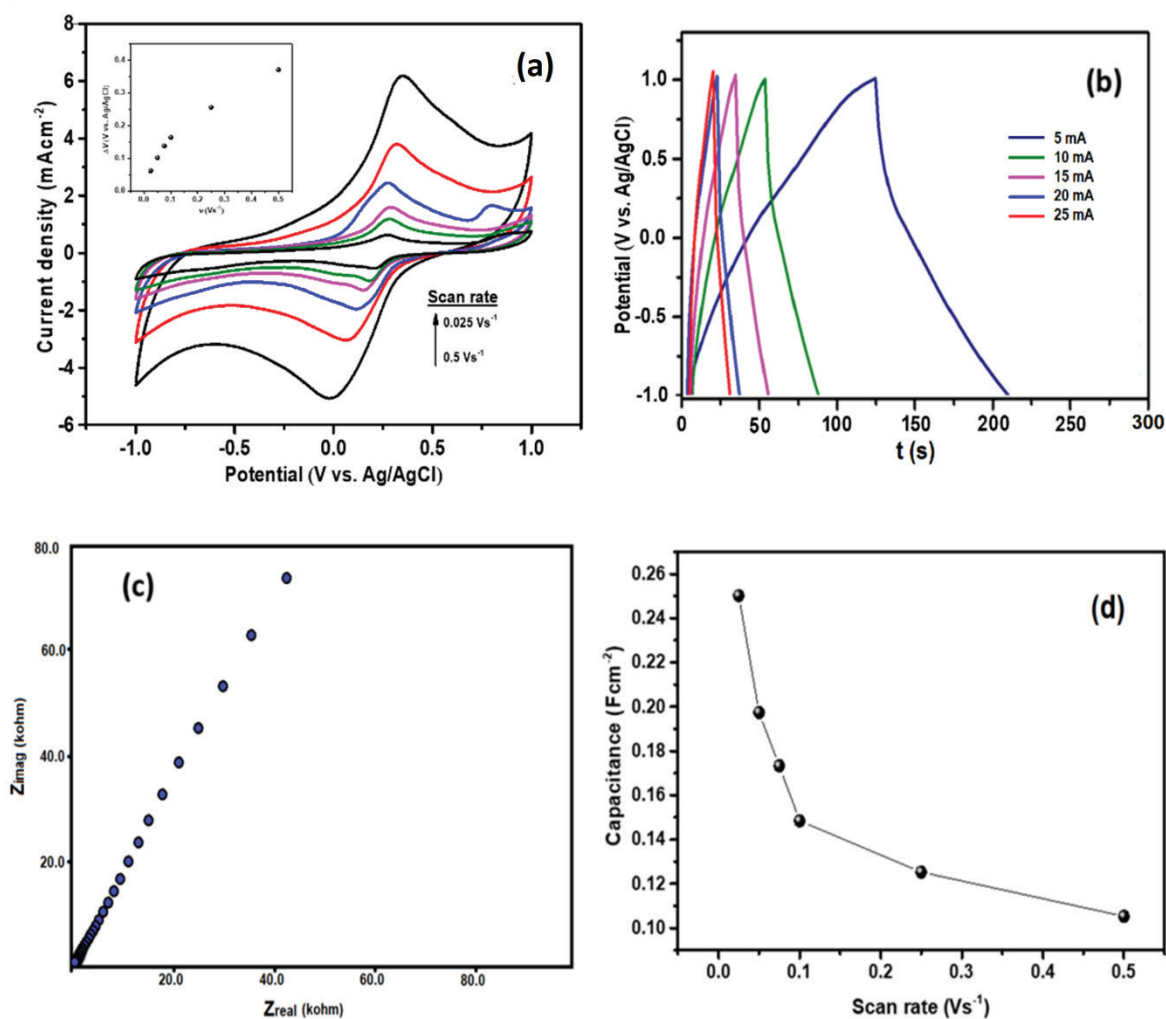


Figure 5. a) Cyclic voltammograms with various scan rates, b) galvanostatic charge-discharge curves with various current, c) electrochemical impedance spectroscopy (0.01 Hz-100 kHz frequency, 10 mV amplitude), d) the change of the capacitance values as a function of scan rates for the ProPpy@rGO-CC electrode in aqueous 0.5 M NaCl electrolyte.

low current density (5 mAcm^{-2}) was applied. For ProPpy@rGO-CC hybrid electrode, the calculated specific capacitance values were 500.4, 394.8, 346.5, 322.1, 250.6, and 210.7 Fg^{-1} at the current densities of 5, 10, 15, 20, and 25 Ag^{-1} , respectively. From the results, it is observed that with increasing current density the discharge time gets lower indicating that the faradaic reaction is a diffusion-controlled process occurring at the material surface.

Electrochemical Impedance Spectroscopy (EIS) is a significant technique used to evaluate and understand the electrical resistance and its related phenomenon. EIS measurements were performed in a frequency range between 100 kHz and 0.01 Hz at open circuit potential (OCP) with an alternating current perturbation of 10 mV. The Nyquist plot of the electrode is shown in Fig 5c. The plot exhibits a linear line in the low frequency region, related to the Warburg impedance, indicating the good electron transfer behavior. In the high frequency region, no semicircle was observed, showing that the charge transfer process increases in the supporting electrolyte during the charging and discharging periods (26). The solution resistance of the electrode was observed at approximately 3 ohm. It is well known that in the presence of rGO, the good electrical conductivity allows to decrease the resistance of charge transfer in the electrode/electrolyte interface. Fig 5d shows the change of areal capacitance as a function of increasing scan rates.

Capacitance retention against number of cycles is an important parameter to evaluate the electrochemical performance for practical energy storage applications. As it is seen from the Fig 6a, the ProPpy@rGO-CC electrode shows 95.4% capacitance retention after 5000 consecutive CV cycles recorded at a scan rate of 2 Vs^{-1} . Fig 6b exhibits Ragone plot which is utilized to compare the performance characteristics of different electrode materials prepared for energy storage devices.

The following equations were used to calculate energy and power densities by using cyclic voltammetry results (27).

$$E = \frac{1}{2} C (\Delta V)^2 \quad (2)$$

$$P = \frac{E}{t} \quad (3)$$

where C is the specific (or areal) capacitance, ΔV is the voltage window, P is the power density, t is the discharge time.

According to these equations, maximum specific energy and specific power were calculated as 278.1 Wh kg^{-1} ($139.2 \mu\text{Whcm}^{-2}$) and of 12.5 kW kg^{-1} (52.7 mWhcm^{-2}), respectively. These results are superior to those of previously published electrode materials, such as CQD-/Ppy-N (0.06 Whcm^{-2} at 8.4 W cm^{-2}) (28); GO/PPy (0.01 Whcm^{-2} at 0.1 Wcm^{-2}) (29); RGO (0.2 mWhcm^{-2} at 50 Wcm^{-2}) (30); nitrogen and sulfur co-doped porous carbon fibers film (N, S

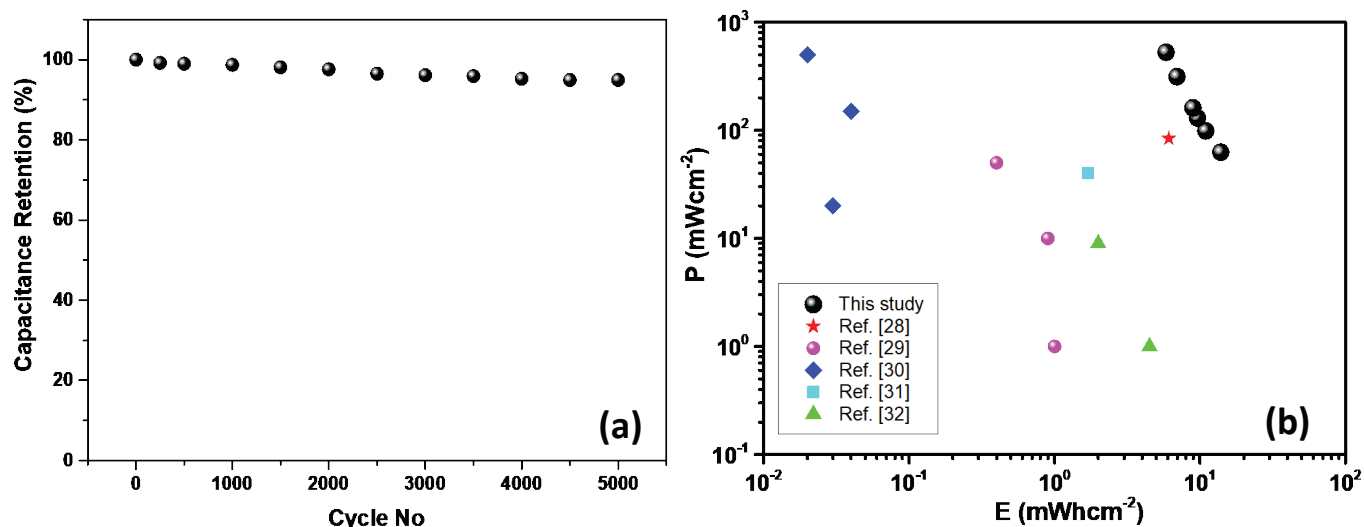


Figure 6. a) Capacitance retention of ProPpy@rGO-CC electrode for 5000 cycles at a scan rate of 2.0 Vs^{-1} , b) Areal Ragone plot showing areal energy and power densities of various electrodes for energy storage systems.

co-doped PCFF) (0.02 Whcm^{-2} at 4 Wcm^{-2}) (31) and graphene/polypyrrole aerogel (GPA) (0.04 Whcm^{-2} at 0.1 Wcm^{-2}) (32).

4. Conclusion

In summary, we have successfully synthesized ProPpy@rGO-CC flexible electrode by using simple two-step hydrothermal method. The morphological and chemical characterization of electrode was clarified by using DRIFTS and AFM techniques. The synthesized ProPpy@rGO-CC electrode showed a maximum specific capacitance of 500.4 Fg^{-1} (215.0 mFcm^{-2}), high specific energy of 278.1 Wh kg^{-1} (139.2 μWhcm^{-2}), and specific power of 12.5 kW kg^{-1} (52.7 mWhcm^{-2}). It is observed that the electrode maintains its initial capacity of 95.4% after 5000 cycles confirming long time cyclic stability at a scan rate of 2.0 Vs^{-1} . The remarkable electrochemical performance can be attributed to the synergistic effect among L-Proline, PPy, and rGO moieties, resulting in abundant electroactive sites and fast diffusion pathways.

Conflicts of interest: The authors report no conflicts of interest.

References

- Guan S, Li J, Wang Y, Yang Y, Zhu X, Ye D, Liao Q. Multifunctional MOF-derived Au, Co-doped porous carbon electrode for a wearable sweat energy harvesting-storage hybrid system. *Adv Mater.* 2023;35(39). doi:10.1002/adma.202304465
- Lv J, Chen J, Lee PS. Sustainable wearable energy storage devices self-charged by human-body bioenergy. *SusMat.* 2021;1(2):285-302. doi:10.1002/sus2.14
- Yin Y, Yang C, Li M, Zheng Y, Ge C, Gu J, Li H, Duan M, Wang X, Chen R. Research progress and prospects for using biochar to mitigate greenhouse gas emissions during composting: a review. *Sci Total Environ.* 2021;798. doi:10.1016/j.scitotenv.2021.149294
- Ahmed S, Sharma P, Bairagi S, Rumjit NP, Garg S, Ali A, Lai CW, Mousavi SM, Hashemi, SA, Hussain CM. Nature-derived polymers and their composites for energy depository applications in batteries and supercapacitors: Advances, prospects and sustainability. *J. Energy Storage.* 2023;66:107391. doi:10.1016/j.est.2023.107391
- Mosa IM. Biosupercapacitors for Implantable Bioelectronics & Portable Microfluidic Devices for Prostate Cancer Biomarker Detection and DNA Damage Screening. 2018.
- Wang T, Wang L, Wu D, Xia W, Zhao H, Jia D. Hydrothermal synthesis of nitrogen-doped graphene hydrogels using amino acids with different acidities as doping agents. *J. Mater. Chem. A.* 2014;2(22):8352-8361. doi:10.1039/C4TA00170B
- Ma G, Yang Q, Sun K, Peng H, Ran F, Zhao X, Lei Z. Nitrogen-doped porous carbon derived from biomass waste for high-performance supercapacitor. *Bioresour Technol.* 2015;197:137-142. doi:10.1016/j.biortech.2015.07.100
- Fu X, Li R, Yan S, Yuan W, Zhang Y, Sun W, Wang X. Porous carbons prepared from polyacrylonitrile doped with graphitic carbon nitride or melamine for supercapacitor applications. *ChemistrySelect.* 2023;8(34). doi:10.1002/slct.202301801
- Wu M, Li W, Li S, Feng G. Capacitive performance of amino acid ionic liquid electrolyte-based supercapacitors by molecular dynamics simulation. *RSC advances.* 2017;7(46):28945-28950. doi:10.1039/C7RA00443E
- Zhou H, Zhou Y, Li L, Li Y, Liu X, Zhao P, Gao B. Amino acid protic ionic liquids: multifunctional carbon precursor for N/S codoped hierarchically porous carbon materials toward supercapacitive energy storage. *ACS Sustainable Chem. Eng.* 2019;7(10):9281-9290. doi:10.1021/acssuschemeng.9b00279
- Sun J, Yu X, Zhao S, Che H, Tao K, Han L. Solvent-controlled morphology of amino-functionalized bimetal metal-organic frameworks for asymmetric supercapacitors. *Inorg Chem.* 2020;59(16):11385-11395. doi:10.1021/acs.inorgchem.0c01157
- Stankovich S, Dikin DA, Piner RD, Kohlhaas KA, Kleinhammes A, Jia Y, Wu Y, Nguyen ST, Rodruoff RS. Synthesis of graphene-based nanosheets via chemical reduction of exfoliated graphite oxide. *Carbon.* 2007;45(7):1558-1565. doi:10.1016/j.carbon.2007.02.034

- 13.** Kang Y, Li W, Ma T, Huang X, Mo Y, Chu Z, Zhang Z, Feng G. Microwave-constructed honeycomb architectures of h-BN/rGO nano-hybrids for efficient microwave conversion. *Compos. Sci. Technol.* 2019;174:184-193. doi:10.1016/j.compscitech.2019.02.029
- 14.** Shahid M, Katugampalage TR, Khalid M, Ahmed W, Kaewsaneha C, Sreearunothai P, Opaprasit P. Microwave assisted synthesis of Mn₃O₄ nanograins intercalated into reduced graphene oxide layers as cathode material for alternative clean power generation energy device. *Sci Rep.* 2022;12(1). doi:10.1038/s41598-022-23622-x
- 15.** Sabari Girisun TC, Saravanan M, Soma VR. Wavelength-dependent nonlinear optical absorption and broadband optical limiting in Au-Fe₂O₃-rGO nanocomposites. *ACS Appl. Nano Mater.* 2018;1(11). doi:10.1021/acsanm.8b01544
- 16.** Schoustra S, Kloots M, Posthuma J, Doorn D, Dijkman J, Smulders M. Raman spectroscopy reveals phase separation in imine-based covalent adaptable networks. *Macromolecules.* 2022;55(23). doi:10.1021/acs.2c01035
- 17.** Chen Z, Takei Y, Deore BA, Nagaoka T. Enantioselective uptake of amino acid with overoxidized polypyrrole colloid templated with l-lactate. *Analyst.* 2000;125(12):2249-2254. doi:10.1039/b005745m
- 18.** Dipojono H, Safitri I, Budi E, Saputro A, David M, Kasai H. Immobilization of amino acids leucine and glycine on polypyrrole for biosensor applications: a density functional theory study. *Itbj Eng Sci.* 2011;43(2):113-122. doi:10.5614/itbj.sci.2011.43.2.4
- 19.** Azioune, A, Chehimi, M, Miksa, B., Basińska, T, Słomkowski, S. Hydrophobic protein-polypyrrole interactions: the role of van der Waals and Lewis acid-base forces as determined by contact angle measurements. *Langmuir.* 2002;18(4):1150-1156. doi:10.1021/la010444o
- 20.** Zhu C, Zhai J, Wen D, Dong S. Graphene oxide/polypyrrole nanocomposites: one-step electrochemical doping, coating and synergistic effect for energy storage. *J. Mater. Chem.* 2012;22:6300. doi:10.1039/c2jm16699b
- 21.** Vleminckx G, Bose S, Leys J, Vermant J, Wübberhorst M, Abdala A, Macosko C, Moldenaers P. Effect of thermally reduced graphene sheets on the phase behavior, morphology, and electrical conductivity in poly[(α -methyl styrene)-co-(acrylonitrile)]/poly(methyl-methacrylate) blends. *ACS Appl. Mater. Interfaces.* 2011;3(8):3172-3180. doi:10.1021/am200669w
- 22.** Bose S, Özdilek C, Seo J, Wübberhorst M, Vermant J, Moldenaers P. Phase separation as a tool to control dispersion of multiwall carbon nanotubes in polymeric blends. *ACS Appl. Mater. Interfaces.* 2010;2(3):800-807. doi:10.1021/am9008067
- 23.** Butt HJ, Cappella B, Kappl M. Force measurements with the atomic force microscope: Technique, interpretation and applications. *J. Surf. Rep.* 2005;59(1-6):1-152. doi:10.1016/j.surfrep.2005.08.003
- 24.** Schirmeisen A, Anczykowski B, Fuchs H. Dynamic modes of atomic force microscopy. In: Bhushan B, editor. *Springer handbook of nanotechnology.* Berlin, Heidelberg: Springer; 2007. p 27. doi:10.1007/978-3-540-29857-1_27
- 25.** Veeramani V, Madhu R, Chen SM, Sivakumar M, Hung CT, Miyamoto N, Liu SB, NiCo₂O₄-decorated porous carbon nanosheets for high-performance supercapacitors. *J. Electacta.* 2017;247:288-295. doi:10.1016/j.electacta.2017.06.171
- 26.** Britto S, Ramasamy V, Murugesan P, Thangappan R, Kumar R. Preparation and electrochemical validation of rGO-TiO₂-MoO₃ ternary nanocomposite for efficient supercapacitor electrode. *Diamond Relat. Mater.* 2022;122:108798. doi:10.1016/j.diamond.2021.108798
- 27.** Ortaboy S, Alper JP, Rossi F, Bertoni G, Salviati G, Carraro C, Maboudian R. MnO_x-decorated carbonized porous silicon nanowire electrodes for high performance supercapacitors. *Energy Environ. Sci.* 2017;10(6):1505-1516. doi:10.1039/C7EE00977A
- 28.** Jian X, Li JG, Yang HM, Zhang EH, Liang ZH. Carbon quantum dots reinforced polypyrrole nanowire via electrostatic self-assembly strategy for high-performance supercapacitors. *Carbon.* 2017;114:533-543. doi:10.1016/j.carbon.2016.12.033

- 29.** Cao J, Wang Y, Chen J, Li X, Walsh FC, Ouyang J, Jia D, Zhou Y. Three-dimensional graphene oxide/polypyrrole composite electrodes fabricated by one-step electrodeposition for high performance supercapacitors, *J. Mater. Chem. A*, 2015;3:14445-14457. doi:10.1039/C5TA02920A
- 30.** Yang C, Zhang L, Hu N, Yang Z, Wei H, Zhang Y. Reduced graphene oxide/polypyrrole nanotube papers for flexible all-solid-state supercapacitors with excellent rate capability and high energy density. *J. Power Sources*. 2016;302:39-45. doi:10.1016/j.jpowsour.2015.10.035
- 31.** Chen L, Wen Z, Chen L, Wang W, Ai Q, Hou G, Li Y, Lou J, Ci L. Nitrogen and sulfur co-doped porous carbon fibers film for flexible symmetric all-solid-state supercapacitors. *Carbon*. 2020;158:456-464. doi:10.1016/j.carbon.2019.11.012
- 32.** Ye S, Feng J. Self-assembled three-dimensional hierarchical graphene/polypyrrole nanotube hybrid aerogel and its application for supercapacitors. *ACS Appl. Mater. Interfaces*. 2014;6(12):9671-9679 doi:10.1021/am502077p


Cite this article: Ortaboy S, Ogretici M, Aras K, Salihi Caliskan E. Amino Acid Supported Conductive Nanocomposite for Developing Flexible Electrode Material for Energy Storage. *Pharmedicine J.* 2024;1(3), 110-120. DOI: 10.62482/pmj.16



Original Article

The Antioxidative, and antimicrobial activity of 2-amino substituted halochalcone N-glycoside derivative compounds

Rezzan Aliyazicioglu¹, Merve Yikilmaz², Seyda Kanbolat¹, Merve Badem¹, Seda Fandakli³,

Sengul Alpay Karaoglu⁴

¹Karadeniz Technical University, Faculty of Pharmacy, Department of Biochemistry, Trabzon, Türkiye

²Karadeniz Technical University, Faculty of Pharmacy, Department of Biochemistry, Trabzon, Türkiye; Haçkalı Baba Devlet Hastanesi, Trabzon, Türkiye

³Artvin Coruh University, Health Services Vocational School, Artvin, Türkiye

⁴Recep Tayyip Erdogan University, Faculty of Arts and Sciences, Department of Biology, Rize, Türkiye

 Corresponding Author: Rezzan Aliyazicioglu (E-mail: rezzan@ktu.edu.tr)

Received: 2024.09.27; Revised: 2024.10.22; Accepted: 2024.10.23

Abstract

Introduction: The aim of this study was to specify the antioxidant and antimicrobial activity synthesized 2-amino substituted halochalcone N-glycoside derivative compounds.

Methods: The antioxidant capacity of synthesized compounds (1-4) was determined by cupric ion reducing antioxidant capacity (CUPRAC), and ferric reducing antioxidant power (FRAP). Antimicrobial activity was determined on 9 microorganism by agar well diffusion method.

Results: According to the study results, compound 3 showed the highest antioxidant activity. The compound 3 showed antimicrobial activity against *Yersinia pseudotuberculosis*, *Pseudomonas aeruginosa*, *Candida albicans* while compound 4 showed antimicrobial activity against *Escherichia coli*, *Yersinia pseudotuberculosis*, *Pseudomonas aeruginosa*, *Enterococcus faecalis*, *Bacillus cereus*, *Staphylococcus aureus*.

Conclusion: 2-amino substituted halochalcone N-glycoside derivative compounds could be evaluated in the pharmaceutical and cosmetic fields due to their antioxidant and antimicrobial potential.

Keywords: Antimicrobial activity, antioxidant activity, halochalcone, N- glycoside

1. Introduction

Chalcones, known as sub-members of flavonoids, are the common word given to substances containing the 1,3-diaryl prop-2-en-1-one carbon skeleton (1). Some chalcone species can be obtained from natural sources as well as synthesized (1, 2). Chalcones, which are commonly found in plants but in small

amounts, have important pharmacological activities, which has led researchers to study the synthesis and biological activities of these compounds (3). The interest in chalcone compounds, which have attracted the attention of the scientific world with their industrial, biological and pharmacological properties, is increasing day by day (4). The substituted aromatic rings and functional α,β -

unsaturated carbonyl groups of chalcone compounds are important in terms of their biological activities (2). The functional groups carried by chalcone and its derivatives isolated or synthesized from plants enable them to exhibit biological activities such as anticancer (5), anti-inflammatory (6), antihyperglycemic (7), anti-HIV (8), antifungal (4), antibacterial (6), antioxidant (9), antimitotic (10) and antituberculosis (11). Chalcones have biological activities such as anticancer, anti-inflammatory, antibacterial, antituberculosis, antidiabetic, antioxidant, antimicrobial, antiviral, antimalarial and neuroprotective effects (12).

Nevertheless, there is insufficient information examining the antioxidant, and antimicrobial activities of 2-amino substituted halochalcone N-glycoside derivative compounds in the literature. That is why antioxidant, and antimicrobial activity of the compounds were examined in present study.

2. Methods

2.1. Chemicals and instrumentation

2,2-Diphenyl-1-picrylhydrazyl (DPPH) were purchased from Sigma-Aldrich (St. Louis, MO, USA). Methanol, ethanol, acetic acid, and acetonitrile were obtained from Merck (Darmstadt, Germany). Trolox (6-hydroxy-2,5,7,8-tetra-methylchroman-2-carboxylic acid), TPTZ (2,4,6-tripyridyl-s-triazine) and Folin-Ciocalteu's phenol reagent were purchased from Fluka Chemie GmbH (Buchs, Switzerland). Ampicillin and Fluconazole were purchased from Mustafa Nevzat and Pfizer, respectively.

2.2. Supply of compounds

The names of the compounds used in the study are given in Table 1. The compounds (1-4) used in the study were synthesized in our previous studies (13) and used in experiments by taking sufficient amounts.

2.3. Antioxidant activity

In order to determine the ferric reduction antioxidant power, FRAP method was performed as stated in the literature (14). Trolox was prepared as standard in a range of concentrations (62.5, 125, 250, 500,

1000 μ M). The methanolic extract and FRAP reagent was added in test tubes. All samples were incubated in dark conditions at 37 °C during 20 minutes. The absorbance was read 595 nm against a blank. CUPRAC method was applied to investigate the cupric ion reducing capacity of the compounds (15). The absorbance of the samples was measured at 450 nm. Whole processes was repeated in triplicate. The CUPRAC values were expressed as μ M Trolox equivalent per gram of sample (15).

2.4. Antimicrobial activity

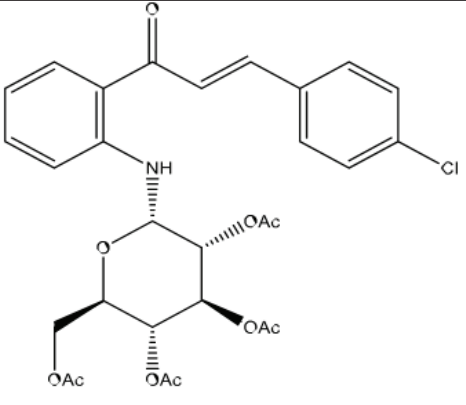
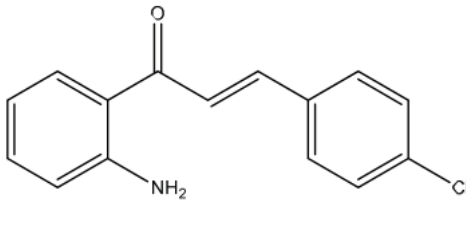
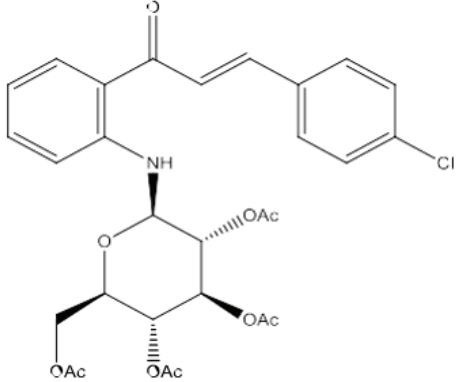
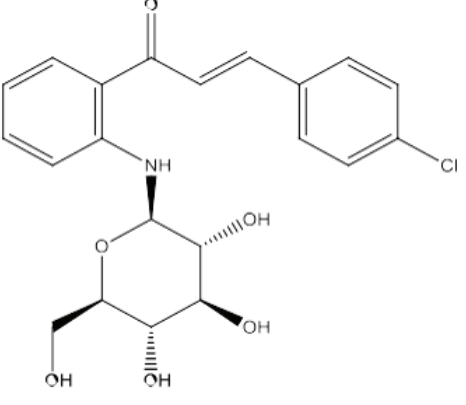
2.4.1. Test microorganisms

All microorganisms used in the study were provided from Refik Saydam Hıfzıssıhha Institute (Ankara, Turkey). *Escherichia coli* ATCC 25922, *Yersinia pseudotuberculosis* ATCC 911, *Pseudomonas aeruginosa* ATCC 43288 from Gram negative bacteria, *Staphylococcus aureus* ATCC 25923, *Enterococcus faecalis* ATCC 29212, *Bacillus cereus* 702 ROMA from Gram positive bacteria, and *Mycobacterium smegmatis* ATCC607 from no Gram were chosen as test bacteria. Moreover, *Candida albicans* ATCC 60193 and *Saccharomyces cerevisiae* RSKK 251 were chosen as yeast.

2.4.2. Antimicrobial assay

In order to detect the antimicrobial activity, some modifications were made in agar well diffusion method (16). Each bacterium was suspended in Mueller-Hinton (MH) broth (Difco, Detroit, MI). Yeast-like fungi were suspended in Yeast extracts broth. Micro-organisms were subsequently diluted to approximately 10^6 colony forming units (cfus) per ml. Potato Dextrose (PD) Agar (Difco, Detroit, MI) was used for yeast-like fungi and Brain Heart Infusion (BHI) Agar for *M. smegmatis* (17). These were first "flood-inoculated" onto the surface of MH and PD agars and subsequently dried. Wells with a diameter of 5 millimeters were opened from the agar using a sterile cork borer and 50 μ L of extract was added to the wells. The plates were then incubated at 35°C for 18 hours. Antimicrobial activity was studied by comparing the zone of inhibition with the test organism. In this study, ampicillin, fluconazole and streptomycin as the standard drug were preferred (16,17).

Table 1. Compounds used in the study

Code of the compound	Full name of the compound	Explicit formulas of compounds
1	<i>(2E)</i> -1-[2-(2,3,4,6-tetra- <i>O</i> -acetyl- <i>N</i> - α - <i>D</i> -glucopyranosyl)phenyl]-3-(4-bromophenyl)prop-2-en-1-on	
2	[(<i>2E</i>)-1-(2-aminophenyl)-3-(4-chlorophenyl)prop-2-en-1-on]	
3	<i>(2E)</i> -1-[2-(2,3,4,6-tetra- <i>O</i> -acetyl- <i>N</i> - β - <i>D</i> -glucopyranosyl)phenyl]-3-(4-bromophenyl)prop-2-en-1-on	
4	<i>(2E)</i> -1-[2-(<i>N</i> - β - <i>D</i> -glucopyranosyl)phenyl]-3-(4-chlorophenyl)prop-2-en-1-on	

2.5. Statistical Analysis

Statistical analysis of all data was evaluated with the Statistics Program for Social and Science (SPSS). Calibration graphs were created according to the absorbance against the concentration of the standard. Experimental results were given as means \pm standard deviation.

3. Results

3.1. Antioxidant activities of compounds

The results of antioxidant activities of the compounds are presented in Table 2. Antioxidant activity of compounds was identified by using two different methods i.e. cupric ion reducing antioxidant capacity (CUPRAC), and reducing antioxidant power (FRAP). The compound 3 showed the highest antioxidant activity. Then compounds 2, 4 and 1 followed in that order. CUPRAC and FRAP results of the compound 3 were found as $172.778 \pm 3.068 \mu\text{M}$ Trolox/g sample and $287.067 \pm 8.994 \mu\text{M}$ Trolox/g sample, respectively.

Table 2. The antioxidant activities of compounds

Test Compounds	CUPRAC ¹	FRAP ²
1	25.139 \pm 1.641	80.733 \pm 5.715
2	93.7501 \pm 1.021	55.733 \pm 3.399
3	172.778 \pm 3.068	287.067 \pm 8.994
4	33.333 \pm 1.483	78.733 \pm 5.907

¹CUPRAC value represents the copper reducing antioxidant power (μM trolox equivalent/gram).

²FRAP value indicates iron reducing antioxidant power (μM trolox equivalent/gram).

3.2. Antimicrobial activities of compounds

While compound 2 showed antimicrobial activity against *E. coli*, *Y. pseudotuberculosis*,

P. aeruginosa, *E. faecalis*, *M. smegmatis* and *C. albicans*, compound 1 showed activity only against *M. smegmatis*. The compound 3 showed antimicrobial activity against *Y. pseudotuberculosis*, *P. aeruginosa*, *C. albicans*. While compound number 4 showed antimicrobial activity against *E. coli*, *Y. pseudotuberculosis*, *P. aeruginosa* among gram negative bacteria, showed activity against *E. faecalis*, *B. cereus*, *S. aureus* among gram positive bacteria (Table 3).

Table 3. Inhibition zone values of compounds

Tested Compounds	Microorganisms and Inhibition Zone (mm)								
	Gram negative			Gram positive			No gram	Yeast Like Fungi	
	Ec	Pa	Yp	Ef	Bc	Sa	Ms	Ca	Sc
1	-	-	-	-	-	-	6	-	-
2	7	6	6	-	6	-	15	6	-
3	-	7	6	-	-	-	-	6	-
4	8	6	8	6	10	7	-	-	-
Ampicillin	10	10	18	10	35	15	-	-	-
Fluconazole	-	-	-	-	-	-	-	25	25
Streptomycin	-	-	-	-	-	-	35	-	-

Q. Ec: *E. coli* ATCC 25922, *Pa:* *P. aeruginosa* ATCC 43288, *Yp:* *Y. pseudotuberculosis* ATCC 911, *Ef:* *E. faecalis* ATCC 29212, *Bc:* *B. cereus* 702 Roma, *Sa:* *S. aureus* ATCC 25923, *Ms:* *M. smegmatis* ATCC607, *Ca:* *C. albicans* ATCC 60193, *Sc:* *S. cerevisiae* RSKK 251, (-): no activity

4. Discussion

Chalcones are an important member of the flavonoid family (18). Many heterocyclic compounds of biological importance such as flavones, pyrazolines and indoles etc. can be synthesized using chalcones. Chalcones consist of a 15-carbon propane chain structure to which two phenyl rings are attached at the 1,3 positions (19). Chalcones containing oxygen atoms in their aromatic ring structure are of great biological importance (20). Chalcones are reported to have a wide range of pharmacological properties such as anticancer, antioxidant, antimalarial, antitubercular, antiviral, anti-inflammatory, antidiabetic, antihistamine, antiulcer and antibacterial (21-24).

It is known that free radicals are the basis of various diseases such as cardiovascular diseases, cancer, chronic inflammation and the like. It has been determined that flavonoid components prevent the formation of these radicals, can prevent lipids from undergoing oxidation by binding metal ions, and can inhibit the enzymatic systems that play a role in the formation of radicals (25). In our study, antioxidant activities of synthesized compounds were measured by using FRAP and CUPRAC determination methods. According to these methods, it was found that compound 3 showed the highest antioxidant activity. FRAP and CUPRAC methods are widely used methods to evaluate the in vitro reducing power of an antioxidant. Various chalcones have

been reported to have high antibacterial activity against gram- positive bacteria. Chalcones have protective effects against many microorganisms. The compounds synthesized in our study were found to have moderate antibacterial and antifungal activity. Particularly, compound 4 was found to exhibit antimicrobial activity against most of the tested microorganisms. Sugamoto et al. investigated the antibacterial activity of the chalcones they synthesized against gram-negative bacteria (*Escherichia coli*, *Proteus mirabilis*, *Pseudomonas fluorescens*) and gram-positive bacteria (*Bacillus subtilis*, *Staphylococcus epidermidis*, *Micrococcus luteus*). They found that not all chalcones were effective against gram- negative bacteria. They found that 4-hydroxyderricin, isobavachalcone, xanthoangelol, xanthoangelol F, bavachalcone and brousochalcone B were active compounds against *Bacillus subtilis*, *Staphylococcus epidermidis*, *Micrococcus luteus* (26). Xanthoangelol and 4-hydroxyderricin isolated from *Angelica keiskei* root were found to exhibit antibacterial activity against *Bacillus subtilis*, *Bacillus cereus*, *Staphylococcus aureus*, *Staphylococcus epidermidis* (27). Kromann et al. showed that the lipophilic character of Licochalcone A is necessary for antibacterial activity (28). Many chalcones have been shown to inhibit the growth of various yeasts and fungi. The antifungal mechanism of action of chalcones is thought to be related to the inhibition of the fungal cell wall. ElSohly et al. evaluated all isolated compounds against the fungal pathogens *Candida albicans* and *Cryptococcus neoformans*. Compound 2, called isobavachalcone, was found to have inhibitory activity against the tested fungal pathogens (29). López et al. showed that chalcones with different substituents in the A and B rings were active against dermatophytes (30).

5. Conclusion

In conclusion, the 2-amino substituted halochalcone n-glycoside derivative compounds we synthesized were shown to have moderate antimicrobial and antioxidant properties. In our opinion, the study is important as it provides a reference for further studies to be conducted with these compounds.

Conflicts of interest: The authors have no conflicts of interest to declare.

Acknowledgements: For funding we acknowledge Karadeniz Technical University Scientific Research Projects Unit (Project No. TYL-2021-9443).

References

1. Climent MJ, Corma A, Iborra S, Velty A. Activated hydrotalcites as catalysts for the synthesis of chalcones of pharmaceutical interest. *J Catal.* 2004;221(2):474-482. doi: 10.1016/j.jcat.2003.09.012
2. Li JT, Yang WZ, Wang SX, Li SH, Li TS. Improved synthesis of chalcones under ultrasound irradiation. *Ultrason Sonochem.* 2002;9(5):237-239. doi: 10.1016/S1350-4177(02)00079-2
3. Erdemoglu N, Sener B. Taksol ve türevlerinin biyosentezi. *Ankara Ecz Fak Derg.* 1999;28(2):99-116. doi: 10.1501/Eczfak_0000000343
4. Lahtchev KL, Batovska DI, Parushev P, Ubiyovoyk VM, Sibirny A. Antifungal activity of chalcones: A mechanistic study using various yeast strains. *Eur J Med Chem.* 2008;43(10):2220-2228. doi: 10.1016/j.ejmech.2007.12.027
5. Mokale SN, Dube PN, Bhavale SA, Sayed I, Begum A, Nevase MC, Shelke VR, Mujaheed A. Synthesis, In-vitro screening, and docking analysis of novel pyrrolidine and piperidine-substituted ethoxy chalcone as anticancer agents. *Med Chem Res.* 2015;24(5):1842-1856. doi: 10.1007/s00044-014-1266-8
6. Ventura TL, Calixto SD, de Azevedo Abraham-Vieira B, de Souza AM, Mello MV, Rodrigues CR, Soter de Mariz e Miranda L, Alves de Souza RO, Leal IC, Lasunskia EB, Muzitano MF. Antimycobacterial and anti-inflammatory activities of substituted chalcones focusing on an anti-tuberculosis dual treatment approach. *Molecules.* 2015;20(5):8072-8093. doi: 10.3390/molecules20058072
7. Satyanarayana M, Tiwari P, Tripathi BK, Srivastava AK, Pratap R. Synthesis and antihyperglycemic activity of chalcone-based aryloxypropanolamines. *Bioorg Med Chem.* 2004;12(5):883-889. doi: 10.1016/j.bmc.2003.12.026
8. Wu JH, Wang XH, Yi H, Lee H. Anti-AIDS agents 54. A potent anti-HIV chalcone and flavonoids from genus *Desmos*. *Bioorg Med Chem Lett.*

- 2003;13(10):1813-1815. doi: 10.1016/s0960-894x(03)00197-5
9. Vogel S, Ohmayer S, Brunner G, Heilmann J. Natural and non-natural prenylated chalcones: synthesis, cytotoxicity and antioxidative activity. *Bioorg Med Chem.* 2008;16(8):4286-4293. doi: 10.1016/j.bmc.2008.02.079
10. Kim DY, Kim KH, Kim ND, Lee KY, Han CK, Yoon JH, et al. Design and biological evaluation of novel tubulin inhibitors as antimetabolic agents using a pharmacophore binding model with tubulin. *J Med Chem.* 2006;49(19):5664-5670. Doi: 10.1021/jm050761i.
11. Lin YM, Zhou Y, Flavin MT, Nie W, Chen FC. Chalcones and flavonoids as anti-tuberculosis agents. *Bioorg Med Chem.* 2002;10(8):2795-2802. doi: 10.1016/S0968-0896(02)00094-9
12. Zhuang C, Zhang W, Sheng C, Zhang W, Xing C, Miao Z. Chalcone: a privileged structure in medicinal chemistry. *Chem Rev.* 2017;117(12):7762-7810. doi: 10.1021/acs.chemrev.7b00020
13. Yikilmaz M, Fandakli S, Sener SO. Newly Synthesized N-Glycosidic Halochalcones Reveal Inhibitory Activity on Pancreatic Triacylglycerol Lipase. *Chem Nat Compd.* 2023;59:629-637. Doi: 10.1007/s10600-023-04075-8
14. Benzie IF, Strain JJ. The ferric reducing ability of plasma (FRAP) as a measure of "antioxidant power": the FRAP assay. *Anal Biochem.* 1996;239(1):70-76. doi: 10.1006/abio.1996.0292
15. Apak R, Güçlü K, Ozyürek M, Karademir SE, Erça E. The cupric ion reducing antioxidant capacity and polyphenolic content of some herbal teas. *Int J Food Sci Nutr.* 2006;57:292-304. doi: 10.1080/09637480600798132
16. Perez C, Pauli M, Bazerque P. An antibiotic assay by the well agar method. *Acta Biol et Med Exp.* 1990;15:113-115.
17. Woods GL, Brown-Elliott BA. Susceptibility Testing of Mycobacteria, Nocardiae, and Other Aerobic Actinomycetes [Internet]. Wayne (PA): Clinical and Laboratory Standards Institute; 2011.
18. Arianingrum R, Arty IS. The effect of bromo chalcone [1-(4'-bromophenyl)-3-(4-hydroxy-3-methoxyphenyl)-2-propene-1-on] on T47D breast cancer cells. *AIP Conf Proc.* 2018;020071. doi: 10.1063/1.5065031.
19. Roleira MFF, Varela CL, Gomes AR, Costa SC, Silva EJT. The health components of spices and herbs: the medicinal chemistry point of view. *Aromatic Herbs in Food Bioactive Compounds, Processing, and Applications.* 2021;35-92. doi: 10.1016/B978-0-12-822716-9.00002-0
20. Eddarir S, Cotellet N, Bakkour Y, Rolando C. An Efficient Synthesis of Chalcones Based on Suzuki Reaction. *Tetrahedron Lett.* 2003;44:5359-5363. doi: 10.1016/S0040-4039(03)01140-7
21. Zhuang C, Zhang W, Sheng C, Zhang W, Xing C, Miao Z. Chalcone: A Privileged Structure in Medicinal Chemistry. *Chem Rev.* 2017;117(12):7762-7810. doi: 10.1021/acs.chemrev.7b00020
22. Sahu NK, Balbhadra SS, Choudhary J, Kohli DV. Exploring pharmacological significance of chalcone scaffold: a review. *Curr Med Chem.* 2012;19(2):209-225. doi: 10.2174/092986712803414132
23. Singh P, Anand A, Kumar V. Recent developments in biological activities of chalcones: a mini review. *Eur J Med Chem.* 2014;85:758-777. doi: 10.1016/j.ejmech.2014.08.033
24. Díaz-Tielas C, Graña E, Reigosa RM, Sánchez-Moreiras A. Biological activities and novel applications of chalcones. *Planta Daninha.* 2016;34:607-616. doi: 10.1590/S0100-83582016340300022
25. Yıldız G, İzli G. Microwave and Convective Drying Methods on Food Drying. Ankara, Turkey: Iksad International Publishing House; 2020. ISBN: 978-6057811-87-5
26. Sugamoto K, Matsusita Y-i, Matsui K, Kurogi C, Matsui T. Synthesis and antibacterial activity of chalcones bearing prenyl or geranyl groups from *Angelica keiskei*. *Tetrahedron.* 2011;67:5346-5353. doi: 10.1016/j.tet.2011.04.104
27. Inamori Y, Baba K, Tsujibo H, Taniguchi M, Nakata K, Kozawa M. Antibacterial activity of two chalcones, xanthoangelol and 4-hydroxyderricin, isolated from the root of *Angelica keiskei* KOIDZUMI. *Chem Pharm Bull.* 1991;39(6):1604-1605. doi: 10.1248/cpb.39.1604
28. Kromann H, Larsen M, Boesen T, Schønning K, Nielsen SF. Synthesis of prenylated benzaldehydes

and their use in the synthesis of analogues of licochalcone A. *Eur J Med Chem.* 2004;39(11):993-1000. doi: 10.1016/j.ejmech.2004.07.004

29. ElSohly HN, Joshi AS, Nimrod AC, Walker LA, Clark AM. Antifungal chalcones from *Maclura tinctoria*. *Planta Med.* 2001;67(1):87-89. doi: 10.1055/s-2001-10621
30. López SN, Castelli MV, Zacchino SA, Domínguez JN, Lobo G, Charris-Charris J, Cortés JC, Ribas JC, Devia C, Rodríguez AM, Enriz RD. In vitro antifungal evaluation and structure-activity relationships of a new series of chalcone derivatives and synthetic analogues, with inhibitory properties against polymers of the fungal cell wall. *Bioorg Med Chem.* 2001;9(8):1999-2013. doi: 10.1016/s0968-0896(01)00116-x

Cite this article: Aliyazicioglu R, Yikilmaz M, Kanbolat S, Badem M, Fandaklı S, Alpay Karaoglu S. The antioxidative and antimicrobial activity of 2-amino substituted halochalcone N-glycoside derivative compounds. *Pharmedicine J.* 2024;1(3):121-127. DOI: 10.62482/pmj.13